agronomy

MDPI

Article

Role of Antioxidant Molecules in the Oxidative Stress Response Networks in the Tangerine Pathotype of *Alternaria alternata*

Xingxing Liang [1,†], Qichen Niu [1,†], Jinchao Kong [1], Xiaoyan Zhao [1], Bin Zhang [2], Lei Li [3], Chen Jiao [2] and Yunpeng Gai [1,*]

[1] School of Grassland Science, Beijing Forestry University, Beijing 100083, China; liangxingx@bjfu.edu.cn (X.L.); niuqichen@bjfu.edu.cn (Q.N.); kongjinchao123@bjfu.edu.cn (J.K.); zhao0223@bjfu.edu.cn (X.Z.)
[2] Institute of Biotechnology, Zhejiang University, Hangzhou 310058, China; a402020763@foxmail.com (B.Z.); biochenjiao@zju.edu.cn (C.J.)
[3] College of Plant Protection, South China Agricultural University, Guangzhou 510642, China; qstlilei@stu.scau.edu.cn
* Correspondence: gaiyunpeng@bjfu.edu.cn
† These authors contributed equally to this work.

Abstract: Antioxidant molecules play a crucial role in maintaining redox homeostasis, eliminating oxidative damage, and regulating pathogenesis in phytopathogenic fungi. These antioxidants function through a complex regulatory network involving enzymatic scavengers such as the superoxide dismutases (SODs), catalases, thioredoxins, and glutathiones, as well as non-enzymatic molecules. Specifically, the thioredoxin and glutathione systems (*AaTrr1*, *AaTsa1*, *AaGpx3*, and *AaGlr1*) mediated by NADPH oxidase represent vital thiol antioxidant systems utilized to regulate the detoxification of reactive oxygen species (ROS) in *Alternaria alternata*. This present study investigated the regulatory roles of *AaBemA*, a component of the fungal NADPH oxidase (*Nox*) complex, in the tangerine pathotype of *A. alternata*. Loss-of-function genetic analysis demonstrated that *AaBemA* is essential for the accumulation of cellular hydrogen peroxide (H_2O_2). Mutant strains with defective *AaBemA* displayed higher sensitivity to H_2O_2 and the ROS-generating oxidant tert-butyl-hydroperoxide. These phenotypes closely resembled those previously observed in *AaNoxB*, *AaTrr1*, *AaTsa1*, *AaGlr1*, and *AaYap1* mutants, suggesting a potential interconnection among them. Notably, the defective phenotype of Δ*AaBemA* could be restored through genetic complementation with wildtype *AaBemA* gene. Subcellular localization of a functional *AaBemA* fused with green fluorescent protein (GFP) gene under confocal microscope revealed a widespread distribution of green fluorescence in the cytoplasm and cell membrane, indicating high expression of *AaBemA* during fungal growth in *A. alternata*. Intriguingly, inactivation of *AaBemA* did not affect the morphological phenotype and pathogenicity, indicating that the *AaBemA* is dispensable for the aforementioned phenotypes. To explore the molecular mechanisms underlying the regulation of ROS stress response, we sequenced the whole transcriptomes of *A. alternata* wildtype and ROS-sensitive mutants (Δ*AaBemA*, Δ*AaNoxB*, Δ*AaGlr1*, Δ*AaTrr1*, Δ*AaTsa1*, Δ*AaYap1*) which displayed considerable sensitivity to oxidants. Comparative transcriptome analysis revealed significant influence on the gene-expression pattern of numerous genes related to glutathione metabolism, cellular oxidant detoxification, cellular response to abiotic stimulus, and cellular response to osmotic stress. The gene-expression data and pathways related to various essential metabolic processes and ROS tolerance enabled us to propose a NADPH oxidase-mediated regulatory network involving NADPH oxidase (*AaNoxB*, *AaBemA*), *AaYap1*, glutaredoxin (*AaGPx3*, *AaGlr1*), and thioredoxin systems (*AaTrr1*, *AaTsa1*) in responding to ROS stress in *A. alternata*.

Keywords: ROS stress response network; antioxidant molecules; redox homeostasis; phytopathogenic fungi; NADPH oxidase; transcriptomics

check for updates

Citation: Liang, X.; Niu, Q.; Kong, J.; Zhao, X.; Zhang, B.; Li, L.; Jiao, C.; Gai, Y. Role of Antioxidant Molecules in the Oxidative Stress Response Networks in the Tangerine Pathotype of *Alternaria alternata*. *Agronomy* **2023**, *13*, 2735. https://doi.org/10.3390/agronomy13112735

Academic Editor: Pedro Javier Zapata

Received: 7 October 2023
Revised: 20 October 2023
Accepted: 28 October 2023
Published: 30 October 2023

Copyright: © 2023 by the authors. Licensee MDPI, Basel, Switzerland. This article is an open access article distributed under the terms and conditions of the Creative Commons Attribution (CC BY) license (https://creativecommons.org/licenses/by/4.0/).

1. Introduction

Plants and pathogens have developed a unique "attack and defense" pattern through long-standing coevolutionary relationship, emphasizing the intertwined and interrelated nature of these developmental processes [1,2]. Numerous biotic (living organisms) such as pathogenic attack, and abiotic (non-living environmental factors) stresses, such as oxidative stress, extreme temperatures, salinity, drought, and heavy metal stress are frequently encountered by plants [3,4]. In response, plants have evolved to develop intricate defense mechanisms including physical barriers, chemical defenses, cell wall fortification, hypersensitive response (HR), systemic acquired resistance (SAR), and phytohormone signaling to combat both biotic and abiotic stresses [5,6]. These defense systems involve the regulation of specific metabolic processes in response to environmental stresses, such as plant hormone regulation, glutathione accumulation, and reactive oxygen species (ROS) production [4,7]. While infected by pathogens, plants quickly recognize pathogen-associated molecular patterns (PAMPs) using pattern-recognition receptors (PRRs) located on the cell membrane to activate pattern-triggered immunity (PTI) that includes the activation of cytoplasmic receptor-like kinases (RLCKs), the mitogen-activated protein kinase (MAPK) signaling pathway, and calcium-dependent protein kinase (CDPK) pathway, and causes ROS burst [8,9]. Among them, ROS are important signaling molecules in the process of plant disease resistance [10]. ROS serve not only as toxic molecules that directly target pathogens but also as signaling molecules that activate immune response pathways [11]. During infection, enzymes known as plant respiratory burst oxidase homologs (RBOHs) can induce programmed cell death of plants, which effectively prevents the spread of pathogens [12,13]. Elevated levels of ROS triggered by RBOHs serve as signals to stimulate the expression of specific genes encoding defense-related proteins and signaling molecules, thereby helping plants to generate an immune response [14,15]. Furthermore, the oxidative burst can cause host plant cells to undergo plant programmed cell death (PCD), as evidenced by the presence of numerous dead spots on the plant leaves [16,17]. Additionally, the generation of ROS has been shown to stimulate the expression of genes involved in plant defense, resulting in the production of chemicals detrimental to the pathogens, suggesting ROS as an effective defensive mechanism for plants to confront diseases [15,18].

Plant pathogens have evolved various strategies to overcome the ROS produced by plants as part of their defense response [19,20]. During infection, pathogens employ a range of strategies, including antioxidant enzymes, the glutathione and thioredoxin systems, metabolic adjustments, efflux pumps, ROS scavengers and quenchers, and ROS-sensitive transcription factors to counteract the plant's oxidative defenses [21,22]. The glutathione and thioredoxin systems are two of the most important thiol antioxidant systems. They collaboratively maintain redox homeostasis and detoxify ROS [23,24]. The thioredoxin pathway encompasses the participation of the thioredoxin protein, thioredoxin reductase, and NADPH, which collaboratively facilitate the reduction in diverse oxidized molecules [25,26]. The glutaredoxin system, which consists of the glutaredoxin protein and glutathione reductase, facilitates the reduction in oxidized glutathione, leading to the transformation of other molecules [27]. Phytopathogenic fungi use these systems to reduce oxidized molecules and protect themselves from oxidative damage. Because of their roles in oxidative damage protein repair, deoxyribonucleotide biosynthesis, protein folding, and sulfur metabolism, thioredoxin and glutaredoxin have received a great deal of attention in the field of science from studies involving filamentous fungi, plants, and human cells. The thioredoxin system serves its intended function by shielding cells from oxidative stress and controlling vital cellular processes like DNA synthesis, cell division, and apoptosis [28,29].

The genus *Alternaria* encompasses approximately 400 species, making it among the most sizable genera within the fungal kingdom. It is a diverse and widespread genus, comprising numerous species known for their ecological and economic importance, particularly as plant pathogens and allergenic agents [30–33]. In particular, the *Alternaria alternata* tangerine pathotype is considered responsible for the Alternaria brown spots (ABS) in citrus, which appear as brown necrotic lesions in young leaves, twigs, and fruits

of citrus [34,35]. Furthermore, *A. alternata* tangerine pathotype can produce the specialized ACT toxin, which cause disease in tangerines, grapefruits, and their respective hybrids. In addition to the synthesis of the ACT toxin, the ability of *A. alternata* tangerine pathotype to detoxify host-generated ROS is crucial for their interaction with host plants. To successfully establish infection, the *A. alternata* tangerine pathotype has evolved sophisticated mechanisms to detoxify or neutralize these ROS. This regulatory network is composed of superoxide dismutases (SODs), catalases, NADPH oxidase (*NoxA*, *NoxB*, *NoxR*), the transcriptional regulator *Yap1*, the mitogen-activated protein (MAP) kinase *Hog1*, the stress-response regulator *Skn7*, thioredoxin (*Tsa1*, *Trr1*), and glutaredoxin systems (*Gpx*, *Glr1*) [23,36]. Previous studies have demonstrated that both *NoxA* and *NoxB* are required for ROS tolerance and virulence, and fungal mutants lacking either of these two parts show dramatically decreased pathogenicity and ROS tolerance. Furthermore, *Yap1*, *Hog1*, and *Skn7* are necessary for detoxifying host-generated ROS in plant pathogens [37], the mutants of which have respective increases in susceptibility to H_2O_2 and various ROS-generating substances [38,39].

In our previous study, we demonstrated that both the thioredoxin and glutaredoxin systems are not only essential for ROS detoxification but also required for pathogenicity in *A. alternata* [23]. Additionally, experimental data have shown that NADPH oxidase (*Nox*) plays a pivotal role in ROS tolerance and pathogenicity in *A. alternata* [19]. However, the underlying regulatory mechanism of these antioxidant systems (thioredoxin system, glutaredoxin system, NADPH oxidase) in *A. alternata* involved in these processes has not been elucidated. In this study, we explored the regulatory role of the *AaBemA* gene, constructing a Δ*AaBemA* mutant. We then conducted a comparative transcriptome analysis between Δ*AaBemA* and the wildtype. Furthermore, we performed a comparative transcriptome analysis between *A. alternata* wildtype and the mutants impaired in NADPH oxidase (*NoxB*), glutathione system (*Glr1*), and thioredoxin system (*Tsa1*, *Trr1*) to better understand the transcriptional responses of these oxidant-sensitive mutants.

2. Materials and Methods

2.1. Fungal Strains and Culture Conditions

A. alternata wildtype strain Z7 was initially collected from the diseased citrus leaves of Wenzhou, Zhejiang Province, China and served as the wildtype in this study [34,40]. The *A. alternata* mutants Δ*AaNoxB*, Δ*AaTsa1*, Δ*AaGlr1*, and Δ*AaTrr1* were generated through targeted deletion of the genes, and they displayed hypersensitivity to ROS stress [23]. For the growth of *A. alternata*, PDA medium containing 200 g potato, 20 g glucose, 20 g agar powder, and 1 L of purified water was used. Meanwhile, for specialized growth conditions or assessments, the V8 medium was used, which comprised 200 g V8 vegetable juice, 3 g calcium carbonate, 20 g agar powder, and 1 L of purified water.

2.2. Construction of Gene Disrupted Mutants

The *AaBemA* gene was disrupted in the *A. alternata* Z7 strain using a split marker approach and protoplast transformation, as previously described [19]. Specifically, the two overlapping truncated segments of the *HYG* gene (*HY/g* and *h/YG*) were, respectively, amplified with primers *M15R* and *hyg5*, and *hyg6* and *M15F*. These fragments were then fused with the 5′ and 3′*AaBemA* fragments, which were separately amplified with primers *BemA-proF* and *M15R:BemA*, and *M15F:BemA* and *BemA-Tail*. Subsequently, a combination of the two fusion products and 10 μL of protoplasts prepared from Z7 strain with polyethylene glycol and $CaCl_2$ were transformed into Petri dishes containing regeneration medium supplemented with 100 μg/mL hygromycin. Putative transformants were identified by PCR. For genetic complementation, a full-length *AaBemA* gene was amplified and fused with the GFP-encoding gene and neomycin-resistant Neo gene. The resultant fragments were then introduced into the protoplasts obtained from Δ*AaBemA* mutant, followed by selection on regeneration medium containing 100 μg/mL G418, and subsequent PCR verifi-

cation. The primers used to generate fragments and for diagnostic PCR can be found in Table S1.

2.3. Fungal Growth Assays and ROS Detection

In order to evaluate the stress tolerance of the fungi, mycelium plugs were cultivated on PDA plates supplemented with chemical agents such as hydrogen peroxide (H_2O_2, 50 mM), tert-butyl-hydroxyperoxide (t-BHP, 2.6 mM), hydrogen peroxide (H_2O_2, 10 mM), cumyl hydrop-eroxide (CHP, 0.8 mM), and diethyl maleate (DEM, 2 mM). After an incubation period of five days at a temperature of 26 °C, the growth-inhibition rate was obtained by gauging the diameter of the colonies on each strain grown in the presence and absence of the varied chemicals. Subsequently, the V8 juice of each strain was incubated at 26 °C for a span of seven days, to assess the productivity of the conidial product. The conidia suspension was then collected in 5 mL of sterile water, and filtered through filter paper for quantification via a hemocytometer under an optical microscope. For the observation and imaging of the fungal strain, a Nikon microscope (Japan) constituting an LV100ND imaging system was utilized, while a Zeiss LSM780 laser confocal microscope (Germany) was used to monitor the fluorescence of GFP. In addition, the mycelium plug was cultivated on PDA for five days and stained by 5 mM 3,3'-diaminobenzidine (DAB) for a duration of twelve hours. The end product of this ROS detection reaction, which manifested as a dark brown polymer, was subsequently examined under the microscope. Finally, to ensure the accuracy of the results, all experiments were conducted twice with each treatment having three replicates.

2.4. RNA Preparation and Transcriptome Sequencing

The *A. alternata* wildtype strain Z7 and its derivative mutants were incubated on PDA plate for 3 days, after which the plugs carrying fungal mycelium were taken from the colony's edge and placed in a triangular flask containing 50 mL of liquid PDB at 25 °C in a shaker. Subsequently, total RNA was deftly extracted with the AxyPrep Multi-Source Total RNA Miniprep Kit (Axygen, Union City, CA, USA) according to the instructions provided by the manufacturer. To evaluate the purity, integrity, and concentration of the RNA, the Spectrophotometer (Kaiao, Beijing, China), Nano 6000 Assay Kit of the Bioanalyzer 2100 system (Agilent Technologies, Santa Clara, CA, USA), and Qubit RNA Assay Kit in Qubit 3.0 were employed, respectively. For RNA-Seq, three biological replicates of each sample were leveraged. The NEBNext UltraTM RNA Library Prep Kit for Illumina (E7530L, NEB, Ipswich, MA, USA) was employed to generate sequencing libraries, which were sequenced on the Illumina NovaSeq6000 platform with 150 bp paired-end reads. Furthermore, the StepOnePlusTM Real-Time PCR System was employed to accurately quantify the qualified insert size (>10 nM).

2.5. Comparative Transcriptome Analysis

The genomic sequence of *A. alternata* strain Z7 was used as the reference genome (http://www.zjudata.com/alternaria/blast.php) (accessed on 29 September 2023) for transcriptome analysis [40]. The raw paired-end read data were then processed by Trimmomatic version 0.36 to remove adapter and low-quality bases [41]. After that, the cleaned reads were mapped to the reference genome using Hisat2 v2.1.0, and a count matrix was generated based on the genes and samples with htseq-count to determine the gene-expression level [42,43]. To uncover differentially expressed genes (DEGs), the R DESeq2 package was utilized while a False Discovery Rate (FDR) of 0.05 and a Log2 Fold Change (FC) higher or equal to 2 were preset. Further, Blast2GO software and eggNOG-mapper database (http://eggnog-mapper.embl.de/) (accessed on 29 September 2023) were used for GO annotations and functional term mapping. AntiSMASH v5.0 was used to search for SM production-related gene clusters which were then visualized with Circos [44,45]. KEGG pathway analysis was performed to map enzymes onto known metabolic pathways, and the statistical enrichment of differential expression genes in KEGG pathways and GO was

carried out by the R package clusterProfiler v4.1.0, with key KEGG pathways being further analyzed by pathview R package. The gene expression of each SM gene clusters were visualized using the R package ComplexHeatmap version 2.6.2 [46]. The gene-expression pattern of the ACT toxin gene cluster in different mutants was visualized using the R package genoPlotR v0.8.11 [47]. Finally, weighted gene co-expression network analysis (WGCNA) was carried out with the R package WGCNA v1.70.3 to explore the genetic interactions and the altered gene sets among mutants and wildtype strain Z7, respectively. The co-expression gene network was demonstrated by the R ggnet v 0.1.0 package [48].

2.6. Pathogenicity Assays

For pathogenicity assays, a 5 mm mycelial plug taken from the PDA media was inoculated onto healthy, detached citrus leaves [49]. Each strain was appraised on at least 15 leaves and experiments were repeated twice. After inoculation, the leaves were placed in a 26 °C incubator for hydrating cultivation for four days, and then observed and photographed.

2.7. Quantitative RT-PCR Analysis

The relative expression levels of differentially expressed genes (DEGs) were analyzed using quantitative real-time PCR (qRT-PCR). Primers for qRT-PCR were designed using Primer-BLAST of NCBI. The *AaActin* gene was used as an internal control. qRT-PCR was performed with SYBR qPCR Master Mix (Vazyme Biotech) on a QuantStudio™ 6 Flex Real-Time Quantitative PCR System (Applied Biosystems, CA, USA) according to the manufacturer's instructions. Three independent biological replicates for each sample were analyzed. All of the primers used in this study are listed in Table S2. The relative expression levels of the genes to wildtype after normalization to the actin gene were calculated from three independent reactions using a comparative $2^{-\Delta\Delta CT}$ ("delta-delta Ct") method as previously described [50].

2.8. Statistical Analysis

The significance of the treatments was assessed through analysis of variance, and the means were separated using Duncan's test ($p < 0.05$).

3. Results

3.1. Targeted Disruption of BemA Gene in A. alternata

The *AaBemA* gene in *A. alternata* encodes a protein with 649 amino acids and comprises an open reading frame (ORF) spanning 2201 base pairs (bp), interrupted by three introns of 88, 115, and 48 bp. The *AaBemA* gene shares 99% sequence identity and 40.88% similarity with the *Bem1* gene from *Aspergillus fumigatus* (XP_746598). Structurally, the *AaBemA* gene is a member of the fungal *BemA*-like family, characterized by the presence of three domains: two SH3, one PX, and one PB1 (Figure 1). The *AaBemA* gene was disrupted using a splitting marker approach that involved two overlapping DNA fragments from the selection marker. This strategy was chosen to enhance the efficiency of targeted gene elimination and facilitate homologous integration in the citrus-pathogenic forms of *A. alternata*, achieving a success rate of 100%. The *AaBemA* gene in *A. alternata* was successfully disrupted using two sequential DNA fragments, 5′*BemA*::5′*HY/g* and 3′*BemA*::3′*h/YG*, sourced from the Hygromycin Phosphotransferase Gene (HYG) cassette, which were introduced into wildtype *A. alternata* protoplasts. Screening of transformants on hygromycin-containing culture medium identified approximately 20 fungal transformants. Further analysis was concentrated on transformants B3 and B6, utilizing both external and internal primer pairs in PCR (Figure 1). For gene-complementation studies, the *AaBemA* gene was amplified and fused with the genes encoding green fluorescent protein (GFP) and neomycin resistance (NEO). Subsequent examination using confocal microscopy confirmed the widespread distribution of green fluorescence in the cytoplasm and on the cell membrane, indicating successful expression of the functionally integrated *AaBemA*-GFP.

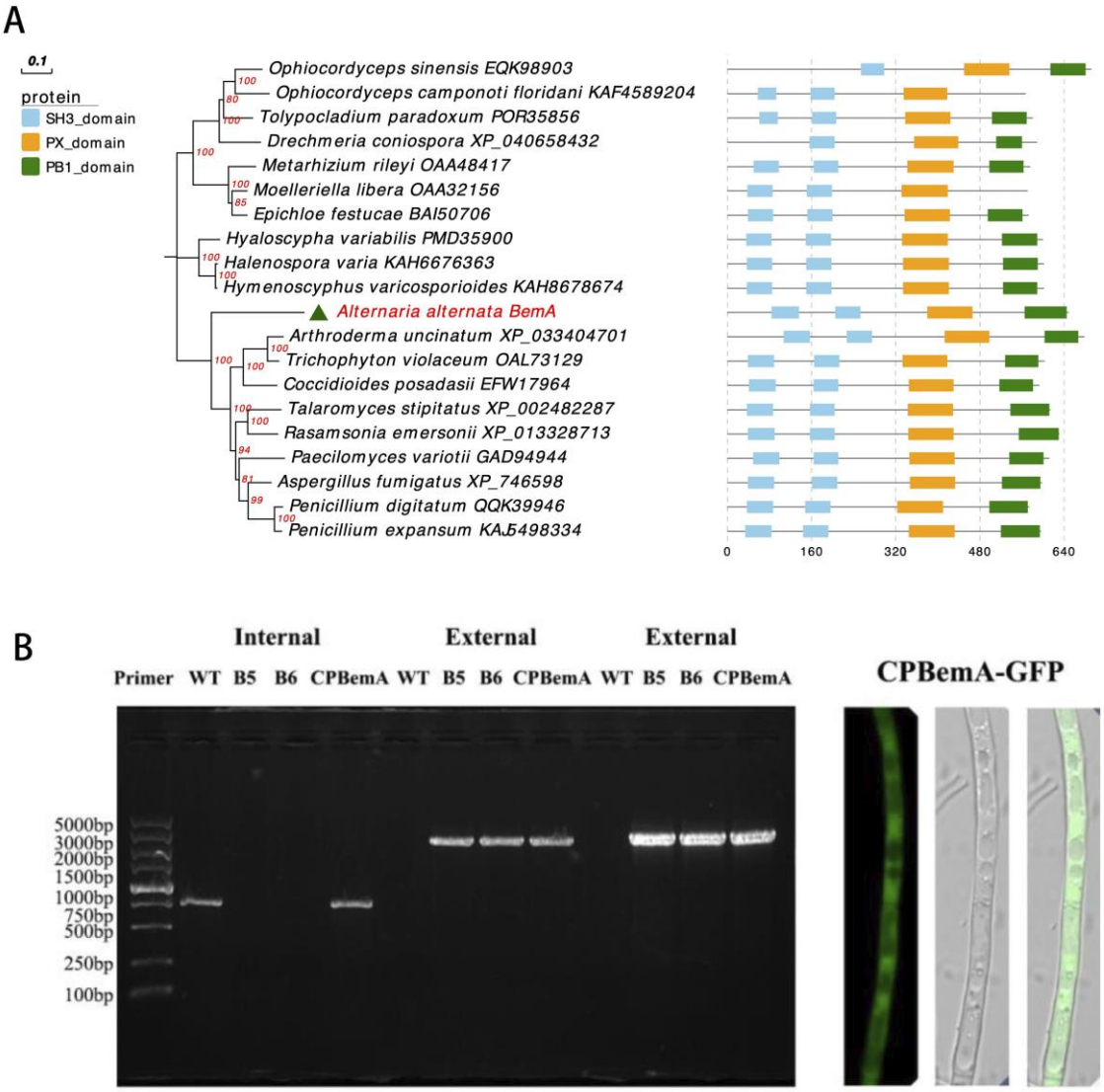


Figure 1. (**A**) Phylogenetic analysis of *BemA* homolog in different fungi. The phylogenetic tree was constructed based on the amino acid sequence alignments of *BemA* protein. These sequences were aligned using ClustalW, and tree construction was performed using the neighbor-joining approach in MEGA7 with 1000 rapid bootstrap replicates. The protein domain was predicated by InterPro (http://www.ebi.ac.uk/interpro/) (accessed on 29 September 2023). The evolutionary tree and its protein domain are illustrated by EvolView v2.0 (https://evolgenius.info/evolview-v2) (accessed on 29 September 2023). (**B**) PCR verification from genomic DNA of wildtype (Z7), two Δ*AaBemA* transformants (B5, B6), *BemA* complemented strain *CPBemA*.

3.2. AaBemA Contributes to the Oxidative Stress Resistance in A. alternata

Phenotypic comparison of the wildtype and Δ*AaBemA* mutant strain did not reveal significant alterations in hyphal morphology, nutrient growth, germination rate, spore yield, or spore morphology (Figure 2). However, the Δ*AaBemA* mutant exhibited heightened sensitivity to tert-butyl hydroxy peroxide (t-BHP) and hydrogen peroxide (H_2O_2), while showing no significant effect on cumyl hydroperoxide (CHP) or diethyl maleate (DEM). This heightened sensitivity of Δ*AaBemA* to elevated ROS is depicted in Figure 3. Restoring functional *AaBemA* under its native promoter in the Δ*AaBemA* mutant reinstated the wildtype tolerance to the tested chemicals, indicating that *AaBemA* is required for the ROS tolerance. Hydrogen peroxide in the fungal colony hyphae was quantified using 3,3′-diaminobenzidine (DAB) staining. A noticeable reduction in H_2O_2 accumulation was

observed in the Δ*AaBemA* mutant compared to the wildtype, as evident from the pigment intensity. Conversely, the complemented strain exhibited deep brown staining, signifying the restoration of H_2O_2 within the hyphae in the complemented strain. Hence, inactivation of *AaBemA* in *A. alternata* led to reduced extracellular and intracellular H_2O_2 accumulation. To ascertain the potential involvement of *AaBemA* in *A. alternata* virulence, infection assays were conducted by inoculating citrus leaves with 5-mm-diameter plugs of either fungal mutants or wildtype fungi. Pathogenicity assays demonstrated that *AaBemA* induced necrotic lesions on citrus leaves at 2 days post-inoculation (dpi), indicating that *AaBemA* is not essential for fungal virulence (Figure 3).

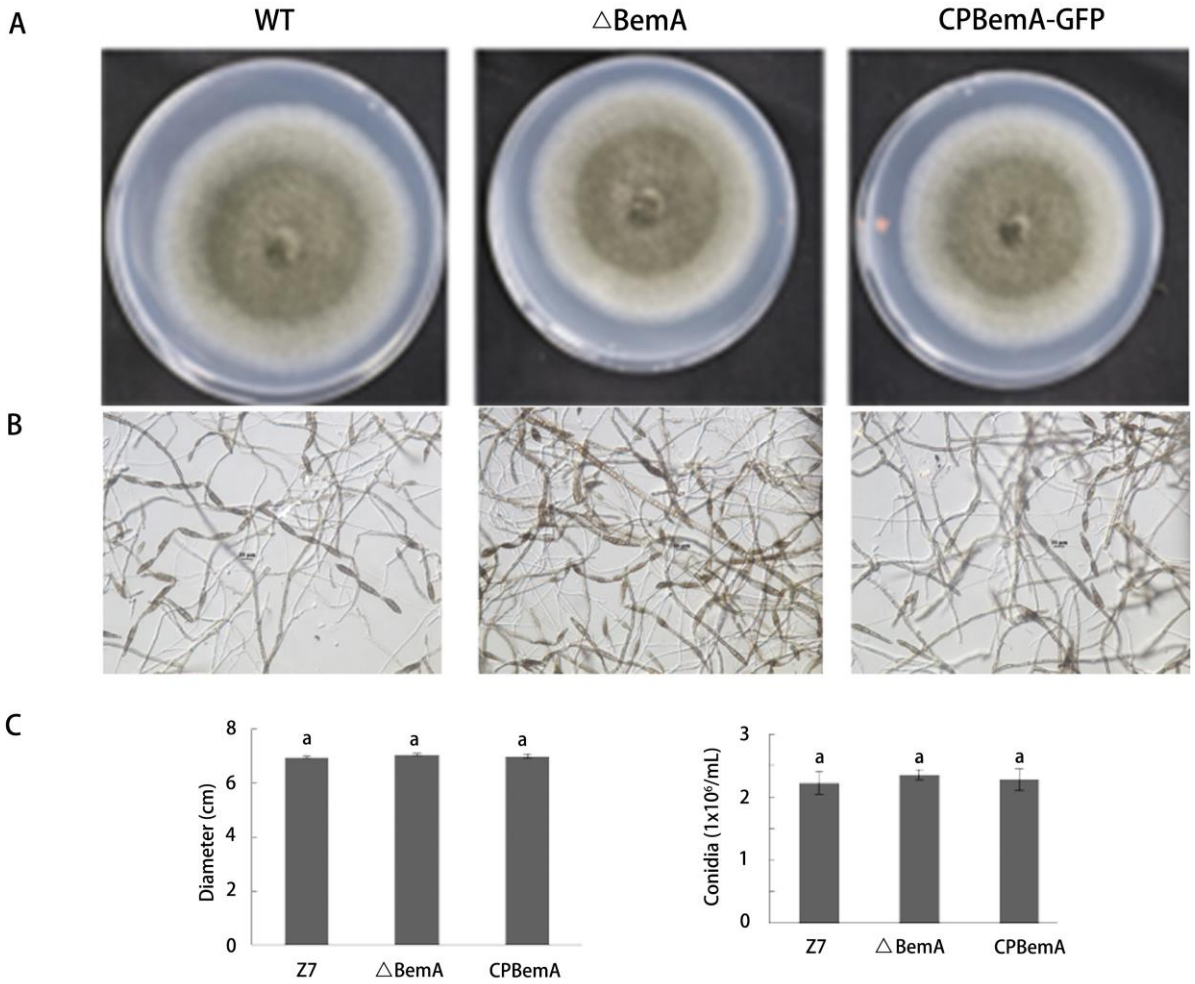


Figure 2. Phenotypic analysis of Δ*AaBemA* mutant showed that the inactivation of *AaBemA* does not affect vegetative development and conidiation of *Alternaria alternata*. (**A**) Morphological characteristics of *A. alternata* wildtype, Δ*AaBemA* mutant, and *CPBemA* mutant strains on PDA at 25 °C in the dark for five days. (**B**) The conidia by *A. alternata* wildtype, Δ*AaBemA* mutant, and *CPBemA* mutant strains photographed under a light microscope. (**C**) The bar plot showed that the inactivation of *BemA* does not affect vegetative growth and conidiation. The different low case letters above columns indicate statistical differences at $p < 0.05$.

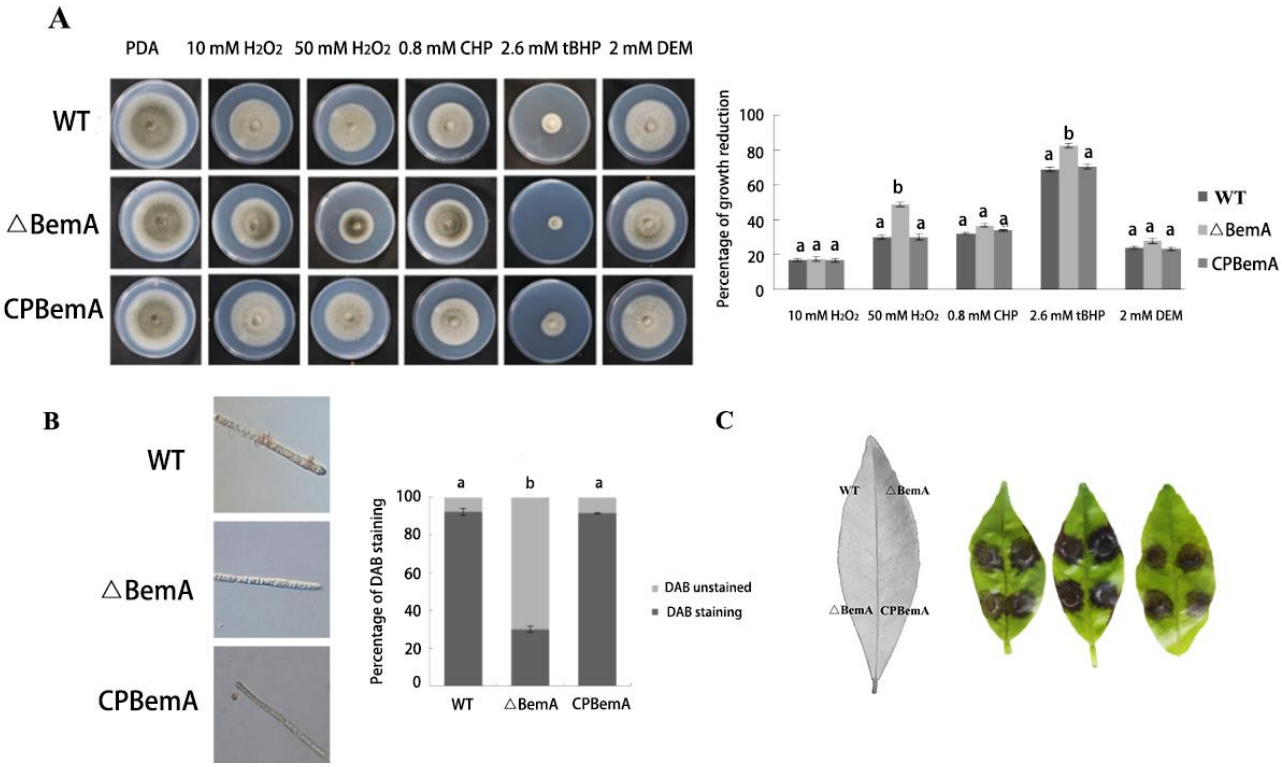


Figure 3. *AaBemA* gene is required for H_2O_2 accumulation and resistance to oxidants in *Alternaria alternata*. (**A**) Growth of the wildtype strain (Z7), Δ*AaBemA* strains with impaired *AaBemA*, the Δ*CPBemA* strain expressing a copy of *AaBemA* cultured on PDA amended with or without 10 mM H_2O_2, 50 mM H_2O_2, tert-butyl-hydroperoxide (t-BHP), cumene hydroperoxide (CHP), or diethyl maleate (DEM) at the indicated concentration is shown. The percentage of growth-reduction determined by comparing a cumulative percentage of the growth of the wildtype and the deletion mutants grown on the same plate is also shown (right). The different low case letters above columns indicate statistical differences at $p < 0.05$. (**B**) The mycelium tip after 12 h of DAB staining indicating that *BemA* is required for H_2O_2 accumulation. The different low case letters above columns indicate statistical differences at $p < 0.05$. (**C**) Pathogenicity was assessed on detached citrus leaves by placing a 5 mm agar plug covering fungal mycelium on the top of the leaves.

3.3. Inactivation of BemA Broadly Affects Many Critical Metabolic Pathways Required for ROS Tolerance

Transcriptome analysis was conducted to investigate the molecular mechanisms underlying *AaBemA* regulation by comparing gene-expression levels between the wildtype and Δ*AaBemA* strains during fungal growth (Figure 4). In total 2708 differentially expressed genes, 998 genes were upregulated and 1710 genes were downregulated in the *BemA*-inactivated strain compared to the wildtype. KEGG enrichment analysis revealed that the inactivation of *AaBemA* significantly downregulated many genes in several important metabolic pathways, including "transporters", "enzymes with EC numbers", "cysteine and methionine metabolism", "GTP-binding proteins", "glutathione metabolism". This suggests *AaBemA*'s involvement in a diverse range of metabolic pathways crucial for ROS tolerance, warranting further investigation to elucidate its specific role in these pathways. GO enrichment analysis revealed the inactivation of *AaBemA* can downregulated many genes associated with various biological processes, including "cellular response to stimulus", "cellular detoxification", "transmembrane transport", "biological regulation", and "cellular response to toxic substance". These analysis indicate that the inactivation of *BemA* can broadly affect many critical metabolic pathways such as glutathione metabolism required for ROS tolerance.

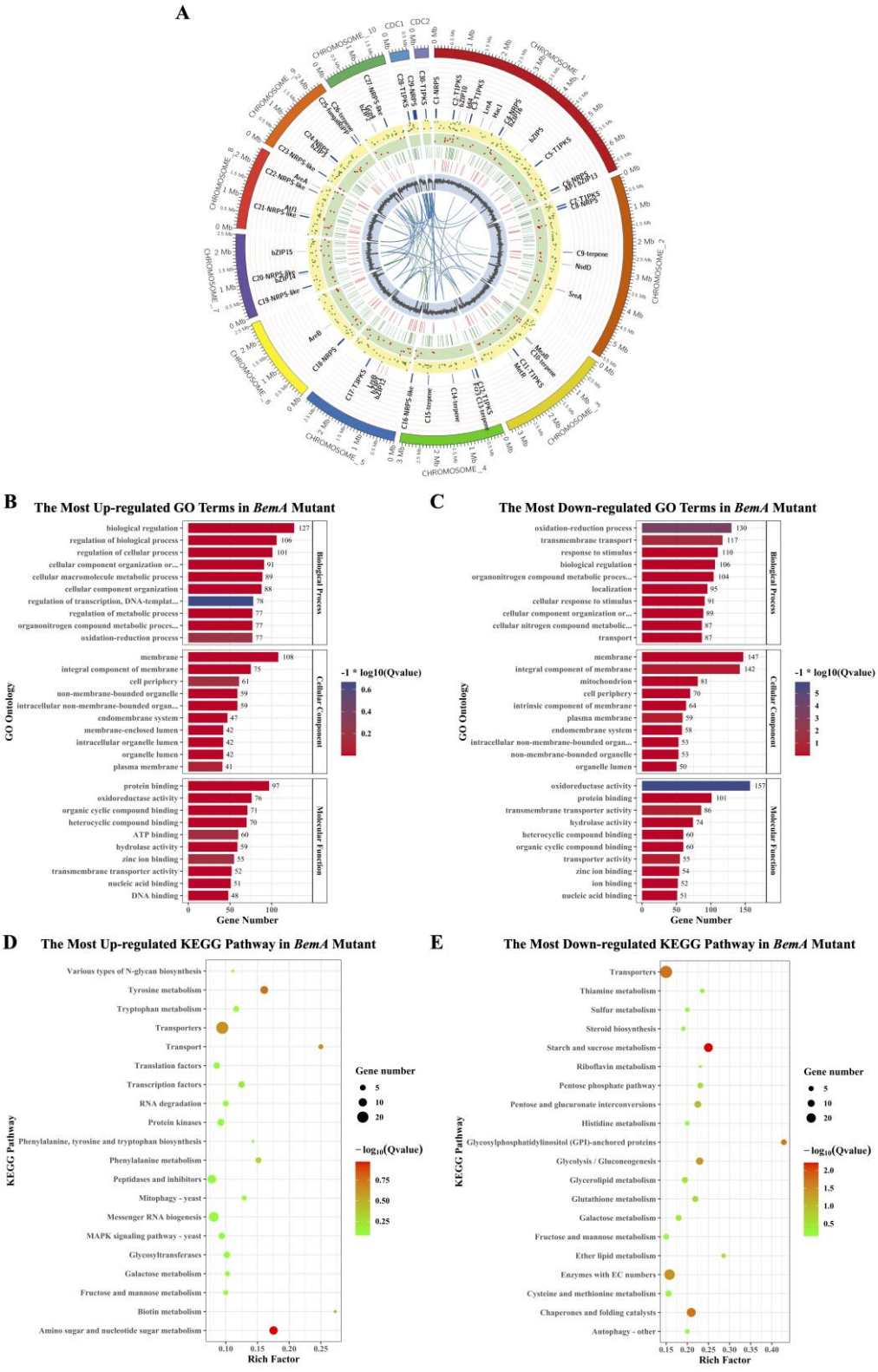


Figure 4. Global regulatory activities of *AaBemA* in *Alternaria alternata* have been revealed by transcriptome analysis. (**A**) Circos plots depict the differential expression of genes (DEGs) between the wildtype strain (Z7) and Δ*AaBemA* mutant. Each circle from the outer periphery to the center represents the following: chromosomal location; secondary metabolite gene clusters; differentially expressed genes (DEGs); GC content; and gene duplications are displayed in the center. (**B**) Gene Ontology (GO) enrichment analysis of the upregulated genes between Δ*AaBemA* and wildtype.

(**C**) Gene Ontology (GO) enrichment analysis of the downregulated genes between Δ*AaBemA* and wildtype. (**D**) KEGG pathway enrichment analysis of the upregulated genes between Δ*AaBemA* and wildtype. (**E**) KEGG pathway enrichment analysis of the downregulated genes between Δ*AaBemA* and wildtype. The count represents the numbers of differentially expressed genes annotated in the pathway term. Rich Factor represents the ratio of numbers of differentially expressed genes annotated in the pathway term to the numbers of all genes annotated in the same pathway. The Q-value is the adjusted *p*-value.

3.4. Inactivation of Glr1 Significantly Affected Multiple Critical Metabolic Pathways Required for Oxidative Stress Response and Redox Homeostasis

Previous studies indicate that the enzyme glutathione reductase (*Glr1*) plays a crucial role in the antioxidant defense mechanisms deployed by pathogenic fungi to protect themselves from the oxidative stress imposed by the host plant. To deepen our understanding of the DEGs associated with the deactivation of *AaGlr1*, GO, and KEGG analyses were conducted to compare DEG expressions between the wildtype and Δ*AaGlr1* mutant stains. These analyses sought to elucidate the role of *AaGlr1* in growth, conidiation, ROS detoxification, resistance to NaCl, resistance to sorbitol, and resistance to mancozeb in *A. alternata*. In total, 4471 differentially expressed genes, including 2059 upregulated genes and 2412 downregulated genes were identified between Δ*AaGlr1* the wildtype (Figure 5). GO enrichment analysis revealed that the inactivation of glutathione reductase (*AaGlr1*) significantly downregulated the expression of numerous genes associated with "transmembrane transport", "oxidation-reduction process", "biological regulation", "response to stimulus", and "localization" (Figure 6). KEGG enrichment analysis revealed that inactivation of *AaGlr1* significantly downregulated the expression of many genes enriched in "transporters", "glutathione metabolism", and multiple critical metabolism pathways (Figure 7). The results demonstrate that the inactivation of *AaGlr1* significantly upregulates 10 genes and downregulates 9 genes in glutathione metabolism, playing a crucial role in regulating the expression of genes related to ROS tolerance. To validate the RNA-Seq findings, a quantitative RT-PCR was conducted. Five genes were randomly chosen for the RT-PCR. While some slight fold-change variations were noted, their expression profiles aligned with the RNA-Seq data (Figure 8).

3.5. Inactivation of Trr1 Broadly Affects Many Critical Metabolic Pathways Required for ROS Tolerance

The thioredoxin system, a network of proteins and enzymes, is pivotal in maintaining cellular redox balance and regulating various cellular processes, underscoring its role in the survival, virulence, and response to environmental stresses of phytopathogenic fungi. It modulates the activity of key enzymes and transcription factors, influencing fungal growth, development, and pathogenicity. To further analyze the gene-expression pattern of mutants with inactivated thiol antioxidant system (*AaTrr1*), this study compared the transcriptomes of Δ*AaTrr1* mutant and *A. alternata* wildtype. In total, 4029 differentially expressed genes, including 1748 upregulated genes and 2281 downregulated genes were identified between Δ*AaTrr1* and wildtype (Figure 5). GO enrichment analysis showed that the inactivation of *AaTrr1* can significantly downregulated the expression of a large number of genes that were enriched in "transmembrane transport", "cellular response to stimulus", "regulation of biological process", "response to chemical", "regulation of cellular process", "cellular nitrogen compound metabolic process", and "response to stress" (Figure 6). KEGG enrichment analysis revealed that the inactivation of *AaTrr1* significantly downregulated the expression of many genes enriched in the "transporters", "exosome", "DNA repair and recombination proteins", and "mitochondrial biogenesis" (Figure 7). Comparative transcriptome analysis demonstrated that *AaTrr1* plays an important role in the regulation of various cellular processes, including DNA synthesis, protein folding, cell-cycle progression, and multiple critical metabolisms related to ROS tolerance.

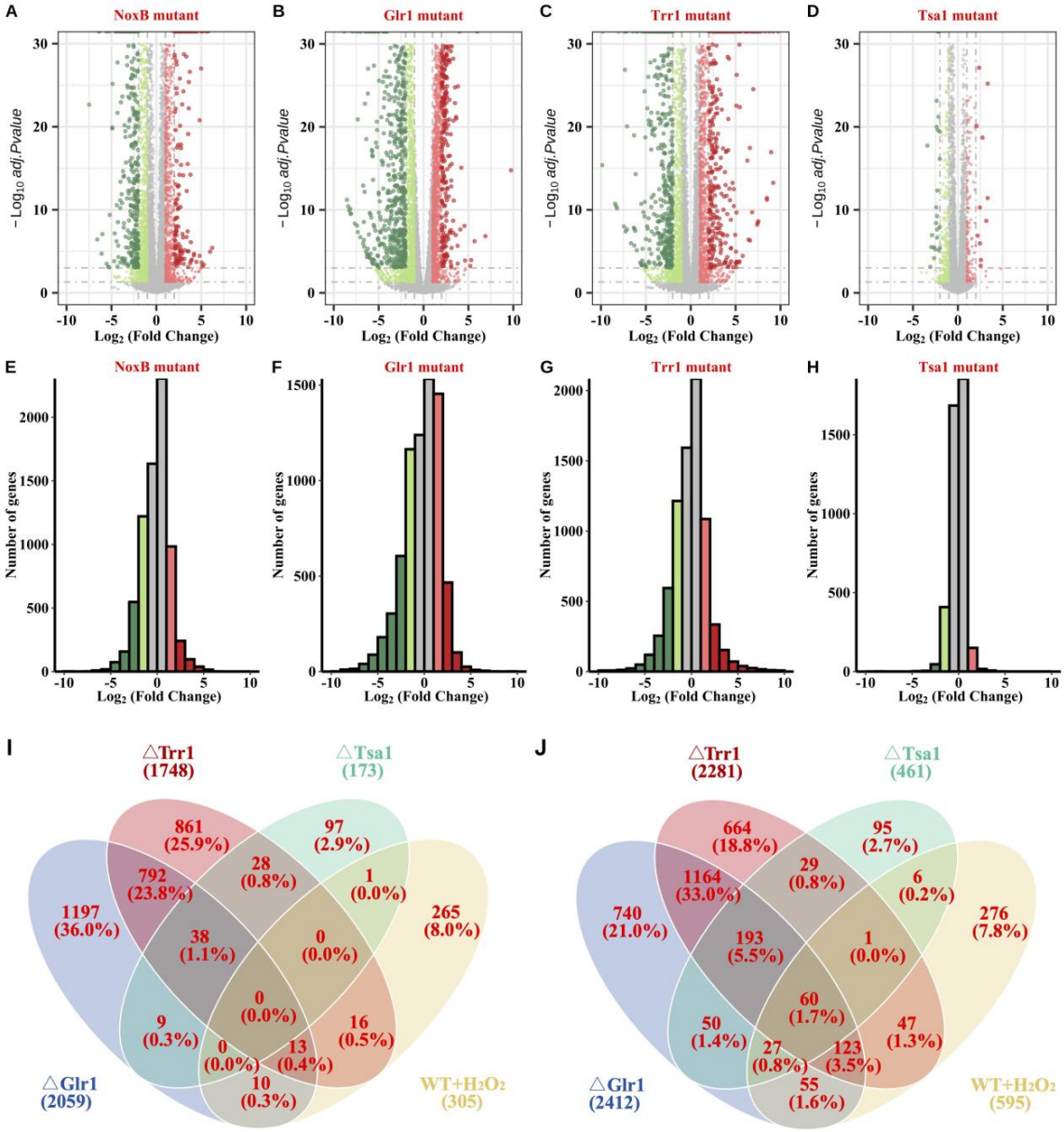


Figure 5. The global gene-expression pattern of four *Alternaria alternata* ROS-sensitive mutants in transcriptome profiles. (**A**) The volcano plot of the gene-expression pattern of *A. alternata* Δ*AaNoxB*. In the volcano plot, the y-axis corresponds to the mean expression value of log10 (adjusted *p*-value, also known as the false discovery rate (FDR)), and the x-axis displays the log2 (fold-change value). The red dots indicate the significantly differentially expressed transcripts (false discovery rate (FDR) < 0.05) which were upregulated under the indicated treatments compared to *A. alternata* (WT); the green dots represent the significantly differentially expressed transcripts (FDR < 0.05) which were downregulated under the indicated treatments compared to *A. alternata* (WT); the grey dots represent the transcripts whose expression levels did not reach statistical significance (FDR > 0.05) or whose absolute value of log2 (fold-change value) is less than 1. (**B**) The volcano plot of the gene-expression pattern of Δ*AaGlr1*. (**C**) The volcano plot of the gene-expression pattern of Δ*AaTrr1*. (**D**) The volcano plot of the gene-expression pattern of Δ*AaTsa1*. (**E**) The histogram plot of the gene-expression pattern of Δ*AaNoxB*. (**F**) The histogram plot of the gene-expression pattern of Δ*AaGlr1*. (**G**) The histogram plot of the gene-expression pattern of Δ*AaTrr1*. (**H**) The histogram plot of the gene-expression pattern of Δ*AaTsa1*. (**I**) Venn diagram describing overlaps of upregulated genes among the mutant strains Δ*AaGlr1*, Δ*AaTrr1*, Δ*AaTsa1* and WT + H_2O_2. (**J**) Venn plot describing overlaps of downregulated genes among the mutant strains Δ*AaGlr1*, Δ*AaTrr1*, Δ*AaTsa1* and WT + H_2O_2.



Figure 6. Comparative Gene Ontology (GO) analysis of the differentially expressed genes (DEGs) between the transcriptome of *Alternaria alternata* wildtype Z7 and its derivative mutants. The results are summarized in three main GO categories (cellular component, molecular function and biological process). The x-axis indicates different mutants. The y-axis indicates the GO term. The color indicates −Log10 (Q value) of each GO term.



Figure 7. Comparative KEGG pathway analysis between the transcriptome of *Alternaria alternata* wildtype Z7 and its derivative mutants under the indicated treatments. The x-axis indicates different mutants. The y-axis indicates the KEGG pathway. Count represents the numbers of differentially expressed genes enriched in the pathway. The q-value is the adjusted P value. The color indicates the rich factors of each pathway.

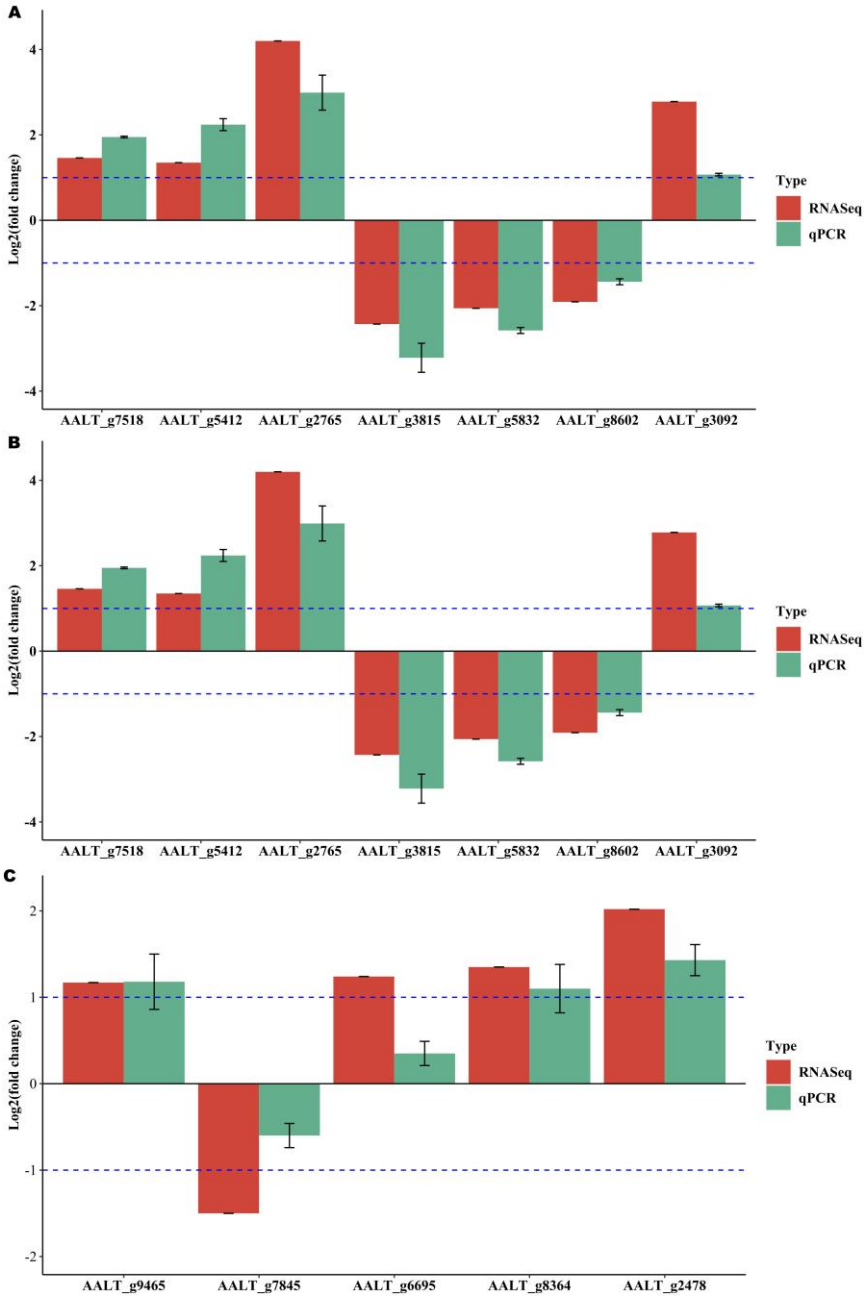


Figure 8. Validation of the RNA-seq data was performed using qRT-PCR in *Alternaria alternata*. The fold-change expression levels were normalized with respect to actin expression levels in each sample, and the data were then presented relative to wildtype expression levels using the $2^{-\Delta\Delta Ct}$ method. (**A**) Relative fold change in the differentially expressed genes between Δ*AaBemA* and wildtype. (**B**) Relative fold change in the differentially expressed genes between Δ*AaNoxB* and wildtype. (**C**) Relative fold change in the differentially expressed genes between Δ*AaGlr1* and wildtype.

3.6. Inactivation of Tsa1 Broadly Affects Many Critical Metabolic Pathways Required for ROS Tolerance

Tsa1 (thiol-specific antioxidant 1), a crucial antioxidant enzyme from the peroxiredoxin family, plays a critical role in cellular protection against oxidative stress by detoxifying harmful ROS and maintaining redox balance. This balance is crucial for normal cellular function, growth, and development of phytopathogenic fungi. *Tsa1* acts as an antioxidant enzyme, specifically scavenging H_2O_2 and other peroxides. By converting ROS to H_2O, *Tsa1* minimizes oxidative damage, ensuring fungal cell survival. In total, 634 differentially

expressed genes, including 173 upregulated genes and 461 downregulated genes were identified between Δ*AaTsa1* and wildtype (Figure 5). To explore the gene-expression pattern of Δ*AaTsa1* mutant, we compared the GO and KEGG enrichment analysis of Δ*AaTsa1* with Δ*AaTrr1* and Δ*AaGlr1*. GO enrichment analysis revealed that the inactivation of *AaTsa1* can significantly downregulate the expression of numerous genes, particularly those involved in the antioxidant process, such as "transmembrane transport", "response to stimulus", "cellular response to stimulus", "regulation of biological process", and "response to stress". KEGG enrichment analysis revealed that the inactivation of *AaTsa1* significantly downregulated the expression of many genes enriched in "chaperones and folding catalysts", "exosome", and "transporters". Although the GO and KEGG enrichment results of Δ*AaTsa1* in *A. alternata* are similar to those of Δ*AaTrr1*, the number of differentially expressed genes is significantly higher in the Δ*AaTrr1* mutant compared to Δ*AaTsa1*. *Tsa1* may collaborate with other antioxidant systems, such as the glutathione and thioredoxin systems, to efficiently counteract oxidative stress. This interplay enhances the overall antioxidant defense capacity of the fungal cell. It can helps phytopathogenic fungi respond to various environmental stresses such as oxidative stress, which is a common challenge faced during plant–fungus interactions or exposure to antifungal agents.

3.7. The Inactivation of Thioredoxin or Glutaredoxin System Significantly Impacts Antioxidant Systems

Analysis of the transcriptomes involving antioxidant pathways revealed significant differential gene-expression upon comparison of the wildtype, wildtype under hydrogen peroxide stress, and wildtype during citrus leaf infection, with Δ*AaTrr1*, Δ*AaTsa1*, and Δ*AaGlr1* mutants. Compared to the wildtype, the mutant strains of Δ*AaTrr1* and Δ*AaGlr1* exhibit significant differential gene expression in antioxidant pathways such as cellular detoxification, cellular response to abiotic stimulus, cellular response to osmotic stress, cysteine and methionine metabolism, glutathione metabolism, and peroxisome. We conducted comparative analysis of the transcriptomes involving the aforementioned antioxidant pathways in the wildtype, wildtype under hydrogen peroxide stress (WT + H_2O_2), wildtype during infection, and Δ*AaTrr1*, Δ*AaTsa1*, and Δ*AaGlr1* mutants. Interestingly, both Δ*AaTrr1* and Δ*AaGlr1* showed contrasting regulation of antioxidant genes compared to their expression during infections. Among the 28 down-regulated genes in both Δ*AaTrr1* and Δ*AaGlr1*, 9 genes were downregulated in the wildtype during the infection process. Among the 31 upregulated genes in both Δ*AaTrr1* and Δ*AaGlr1*, 18 genes were downregulated in the wildtype during the infection process. Many of the upregulated genes in Δ*AaTrr1* and Δ*AaGlr1* were similarly elevated in the wildtype under hydrogen peroxide stress. Among the 31 upregulated genes in both Δ*AaTrr1* and Δ*AaGlr1*, 20 genes were also found to be upregulated under hydrogen peroxide stress in the wildtype.

3.8. Inactivation of AaNoxB Significantly Affected Genes Related to Glutathione Metabolism

NADPH oxidase (*Nox*) are enzymes involved in the generation of ROS, and have diverse functions in cellular processes and pathogenicity in phytopathogenic fungi. During infection, the *Nox* enzyme can produce ROS, such as superoxide anions and hydrogen peroxide, which contribute to the oxidative burst. Previous genetic analyses have elucidated the indispensability of the *Nox* components (*NoxB*) for optimal H_2O_2 accumulation, conidiation, pathogenesis, and resistance to H_2O_2 and other ROS-generating chemicals. The mutant lacking *AaNoxB* (Δ*AaNoxB*) showed heightened sensitivity to H_2O_2 and various ROS-generating oxidants in *A. alternata*. In total, 3404 differentially expressed genes, including 1376 upregulated genes and 2028 downregulated genes were identified between Δ*AaNoxB* and wildtype. To uncover the regulatory role of *AaNoxB*, we compared the GO and KEGG enrichment term of the differentially expressed genes between Δ*AaNoxB*, Δ*AaBemA,* Δ*AaYap1* and *A. alternata* wildtype. GO enrichment analysis revealed that the inactivation of *AaNoxB* significantly downregulated many genes enriched in "transmembrane transport", "biological regulation", "response to stimulus", "regulation of biological

process", and "oxidation-reduction process" (Figure 6). KEGG enrichment analysis revealed that the inactivation of *AaNoxB* significantly downregulated many genes enriched in "transmembrane transport", "oxidation-reduction process", and "iron import into cell" (Figure 7). We also found that the inactivation of *AaNoxB* can downregulate six genes of "glutathione metabolism" including AALT_g41 (GPX2, thioredoxin-like protein, OWY42525, Log2FC = −1.68), AALT_g9652 (GTT1, glutathione transferase, OWY42429, Log2FC = −1.57), AALT_g5306 (hypothetical protein, OWY58155, Log2FC = −1.55), AALT_g7845 (ChaC-like protein, OWY50241, Log2FC = −1.30), and AALT_g8327 (GSH1, glutamate-cysteine ligase, OWY45365, Log2FC = −1.21), indicatingt that the inactivation of *AaNoxB* gene affects various ROS detoxification pathways, particularly surrounding glutathione metabolism in *A. alternata*.

3.9. Multiple Critical SM Gene Clusters Were Affected in A. alternata Mutants

Fungal secondary metabolites are a diverse group of compounds, including but not limited to polyketides, non-ribosomal peptides, terpenoids, alkaloids, and phenolic compounds. Secondary metabolites play a pivotal role in the virulence, pathogenicity, and adaptation in phytopathogenic fungi. *A. alternata* can produce various secondary metabolites with significant ecological functions that allow them to adjust to various conditions. To investigate the gene-expression patterns of secondary metabolite gene clusters affected by the disruption of each gene, we evaluated the transcriptional responses of 30 biosynthetic gene clusters in *A. alternata* mutant. Overall, comparative SM gene cluster analysis demonstrated that multiple critical SM gene clusters were affected in *A. alternata* mutants (Figure 9A). Specifically, the result showed that the inactivation of *BemA* significantly affected the expression of many genes enriched in the "c18_NRPS", "c5_T1PKS (Alternapyrone)", "c16_NRPS_like", "c6_NRPS (Dimethyloprogen)", "c10_terpene", "c11_T1PKS", "c12_T1PKS", "c13_terpene", "c17_T3PKS", "c19_NRPS_like (Phomopsins)", "c1_NRPS", "c20_NRPS_like", "c21_NRPS_like", "c23_NRPS_like", "c24_NRPS", "c25_fungalRiPP", "c27_NRPS_like", "c28_T1PKS (Mellein)", "c29_NRPS (ACT_Toxin I)", "c2_T1PKS (Alternariol)", "c3_T1PKS (Melanin)", "c4_NRPS", "c8_NRPS (Equisetin)". The results showed that the inactivation of *BemA* can significantly downregulate the AALT_g11748 (metalloprotease, OWY54920), AALT_g11758 (Aft11-1, OWY54930), AALT_g11749 (ACTTS4, acetyl-CoA synthetase-like protein, OWY54921), AALT_g11754 (ACTR, AktR-1, OWY54926), which are important enzymes in C29_NRPS (ACT_Toxin I) (Figure 9B).

3.10. Comparative Transcriptome Analysis of Genes Related to ROS Stress Response

To further analyze the gene related to ROS stress response, we compare the genes related to critical GO terms including cellular detoxification, cellular oxidant detoxification, cellular response to abiotic stimulus, cellular response to osmotic stress (Figure 10). Interestingly, we identified multiple critical genes related to stress response including AALT_g6923 (OWY55320, YCF1, ABC transporter transmembrane region), AALT_g3324 (OWY52959, GLO2, Hydroxyacylglutathione hydrolase C terminus), AALT_g8327 (OWY45365, GSH1, Glutamate cysteine ligase), AALT_g1812 (OWY45365, TSA1, C terminal domain of 1 Cys peroxiredoxin), AALT_g41 (OWY42525, GPX2, belongs to the glutathione peroxidase family), AALT_g2814 (OWY52449, CCP1, belongs to the peroxidase family), AALT_g3416 (OWY53051, Thioredoxin-like domain), AALT_g9686 (OWY58363, TRX1, Thioredoxin), AALT_g11306 (OWY49843, ECM4, Glutathione S transferase), AALT_g1523 (OWY41770, katG, belongs to the peroxidase family. Peroxidase catalase subfamily), AALT_g3238 (OWY52873, TTR1, Glutaredoxin), AALT_g7769 (OWY50165, TRR1, belongs to the class II pyridine nucleotide disulfide oxidoreductase family), AALT_g9933 (OWY52089, cat1, occurs in almost all aerobically respiring organisms and serves to protect cells from the toxic effects of hydrogen peroxide), AALT_g8994 (OWY51721, occurs in almost all aerobically respiring organisms and serves to protect cells from the toxic effects of hydrogen peroxide), AALT_g2809 (OWY52444, GLR1, belongs to the class I pyridine nucleotide disulfide oxidoreductase family), AALT_g9819 (OWY58496, CDC14, dual specificity pro-

tein phosphatase), AALT_g10625 (OWY48180, UME6, fungal specific transcription factor domain), AALT_g789 (OWY43273, SSA2, belongs to the heat shock protein 70 family), AALT_g2857 (OWY52492, CRZ1, C2H2 type zinc finger), AALT_g8966 (OWY54423, DNA polymerase delta), AALT_g8 (OWY42492, MgPP2CL-1, Serine/threonine phosphatases), AALT_g3685 (OWY44820, TIF34, component of the eukaryotic translation initiation factor 3 complex), AALT_g6731 (OWY55128, RAD14, XPA protein C terminus), AALT_g9542 (OWY42319, PSD1, catalyzes the formation of phosphatidylethanolamine), AALT_g9320 (OWY57174, YPD1, Histidine Phosphotransfer domain), AALT_g10096 (OWY49315, HOG1, Mitogen activated protein kinase), AALT_g1775 (OWY42022, RGD1, Fes/CIP4 homology domain), AALT_g912 (OWY43396, YAP1, Transcription factor PAP1), AALT_g3133 (OWY52768, Methyltransferase domain), AALT_g4824 (OWY57673, HRQ1, DNA replication factor CDT1 like), AALT_g8419 (OWY45457, srk1, Serine/Threonine protein kinases), AALT_g3948 (OWY45083, RFC5, DNA polymerase III), AALT_g5082 (OWY57931, Ptp2, Protein tyrosine phosphatase). This study, employing weighted gene coexpression network analysis (WGCNA), sheds light on the intricate gene coexpression patterns within glutathione metabolism, cysteine, and methionine metabolism, peroxisome, and the oxidative stress response. The findings suggest possible connections between glutathione metabolism and various other metabolic pathways, as illustrated in Figure 11. Therefore, we proposed a NADPH oxidase-mediated regulatory network involved NADPH oxidase (*AaNoxA*, *AaNoxB*, *AaNoxR*, *AaBemA*), *AaYap1*, *AaSkn7*, *AaHog1*, glutaredoxin (*AaGPx3*, *AaGlr1*) and thioredoxin systems (*AaTrr1*, *AaTsa1*) in responding to ROS stress detoxification in *A. alternata* (Figure 12). This regulatory network orchestrates a series of events that help *A. alternata* effectively neutralize and detoxify ROS, ensuring its virulence. Upon encountering oxidative stress, the *Nox* complex generates low levels of H_2O_2 from superoxide. H_2O_2 then acts as a signaling molecule, initiating a transcriptional cascade. Key transcription factors (TFs) *AaYap1*, *AaSkn7*, and *AaHog1* are transcriptionally upregulated and translocated to the nucleus. *AaYap1* and *AaSkn7* detect oxidative stress cues through non-canonical signal transduction pathways. Once activated, they trigger the expression of oxidative stress-responsive genes like *AaTrr1*, *AaTsa1*, *AaGPx3*, and *AaGlr1*, to detoxify H_2O_2. Working in concert with thioredoxin, they cycle between reduced thioredoxin ($TRX^{[red]}$) and oxidized thioredoxin ($TRX^{[ox]}$). Additionally, *AaGPx3* and *AaGlr1* function with glutathione, cycling between reduced glutathione (GSH) and oxidized glutathione (GSSG), effectively neutralizing H_2O_2. This regulatory network provides insight into ROS regulation and detoxification mechanisms in response to ROS stress.

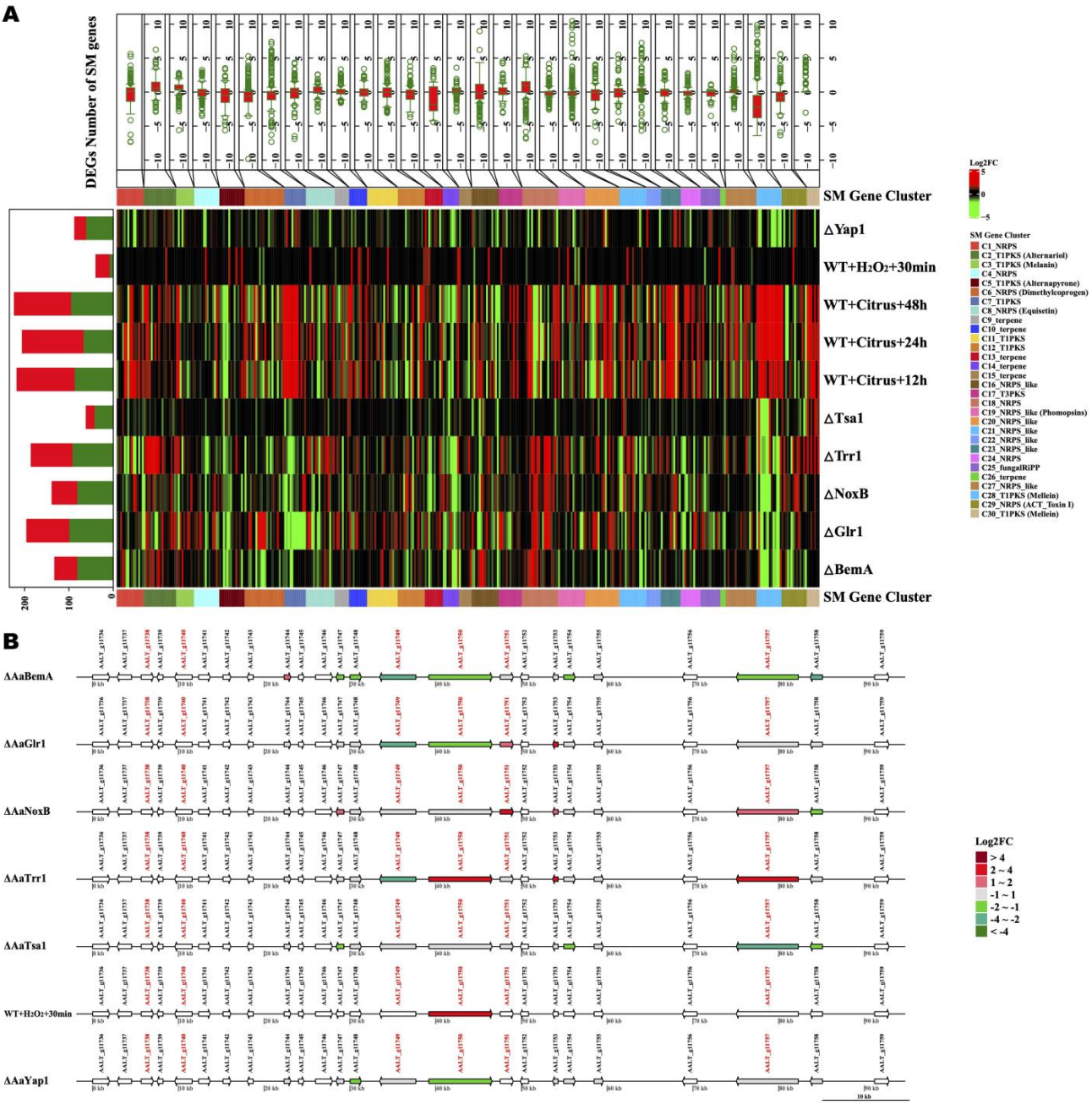


Figure 9. Multiple critical SM gene clusters were affected in *Alternaria alternata* mutants. (**A**) The gene-expression pattern of SM gene clusters the differentially expressed genes (DEGs) between the transcriptome of *A. alternata* wildtype Z7 and its derivative mutants. (**B**) The gene-expression pattern of the ACT toxin gene cluster in its derivative mutants and *A. alternata* wildtype Z7. The text in red represents the core gene of the secondary metabolite gene cluster.



Figure 10. Expression profiles of fungal antioxidant system-related genes in *Alternaria alternata* mutants. Heatmap of differentially expressed genes (DEGs) related to cellular detoxification, cellular oxidant detoxification, cellular response to abiotic stimulus, cellular response to osmotic stress reveals the disparity in gene expression in antioxidant mutants. The bar graph above the heatmap shows the DEGs for each treatment. The bar graph on the right displays the DEGs for each gene. Red symbolizes upregulation; gray indicates no differential expression; green stands for downregulation. The asterisk in the heatmap implies that Log2FC is greater than or equal to 1.0 or less than or equal to −1.0, while the false discovery rate (FDR) is lower than or equal to 0.05.

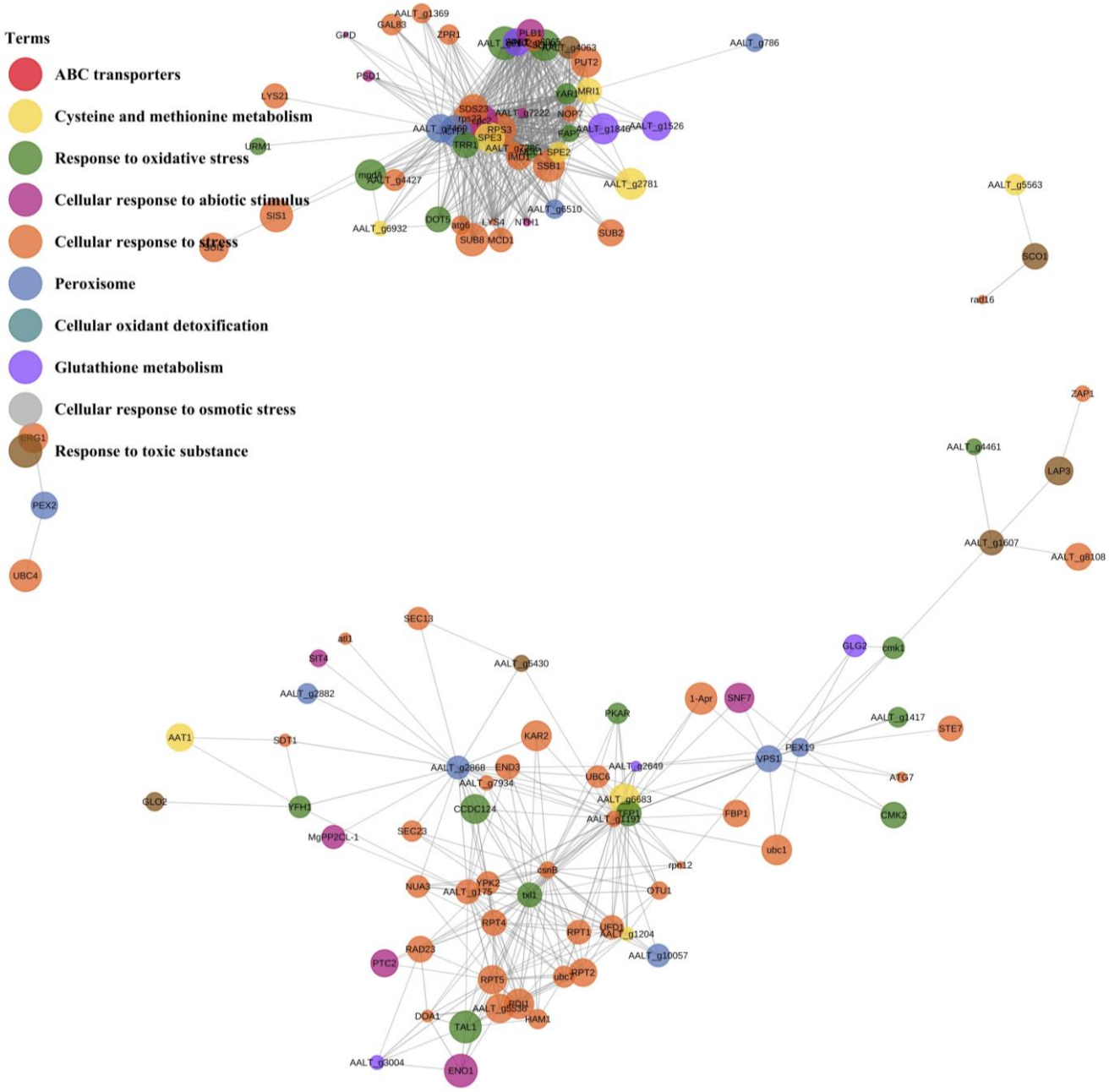


Figure 11. Weighted gene co-expression network analysis (WGCNA) of the genes related to different GO terms in transcriptome profiles. The thresholds of the weight between each gene were ≥0.25 and the color of each gene indicates different GO terms. The gene size in the network indicates the relative expression of each gene.

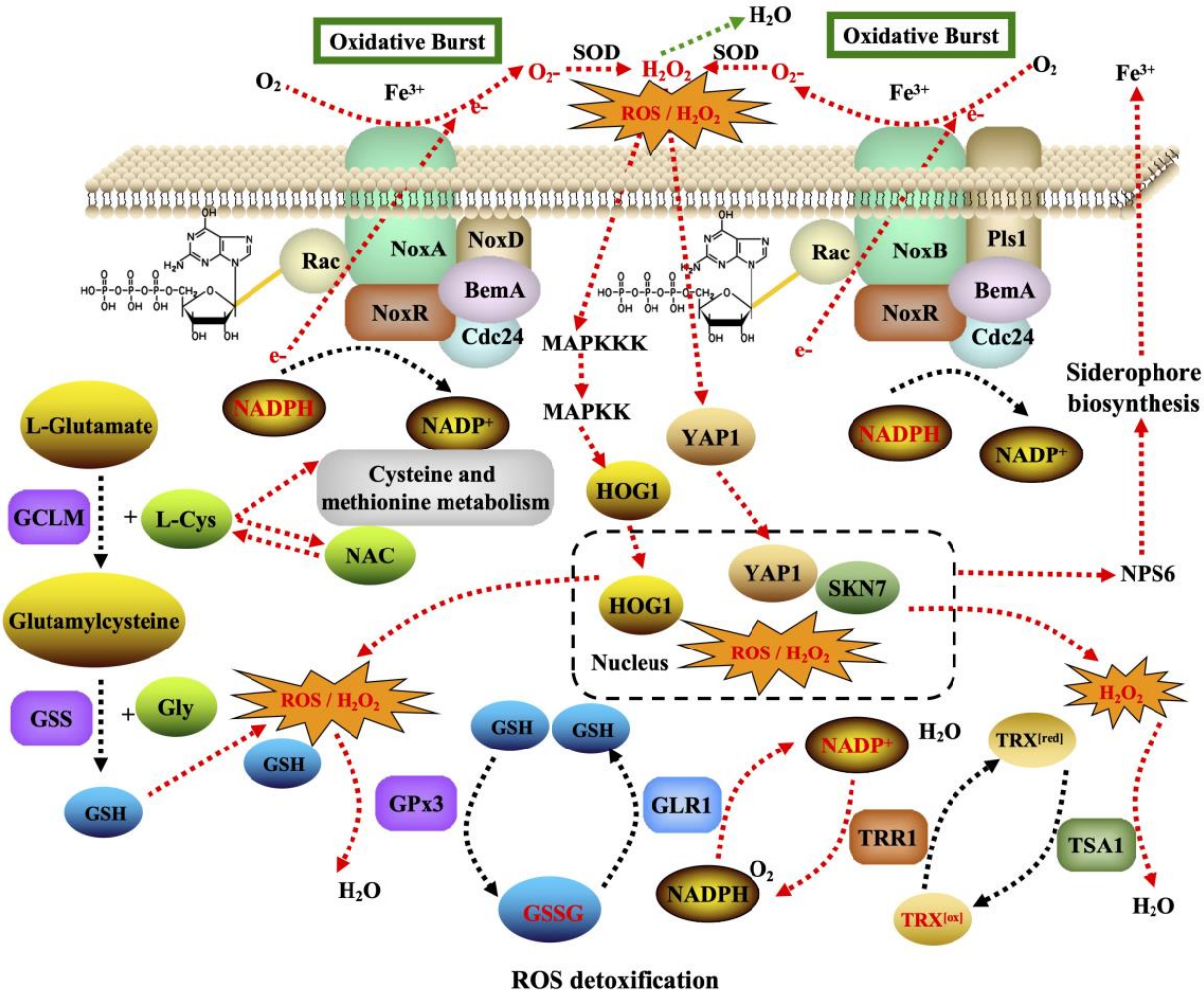


Figure 12. The proposed regulatory network for the fungal antioxidants in *Alternaria alternata* involves a set of key components, including NADPH oxidase (Nox), Yap1, Hog1, Skn7, GPx3, Glr1, Trr1, and Tsa1, in response to reactive oxygen species (ROS). NADPH oxidase generates superoxide (O^{2-}), which is subsequently transformed into hydrogen peroxide (H_2O_2) through superoxide dismutase (SOD). Under various ROS-induced stresses, the stress-responsive regulators Yap1, Hog1, and Skn7 can translocate to the nucleus and modulate the transcription of GPx3, Glr1, Tsa1, and Trr1.

4. Discussion

The ability of phytopathogenic fungi to endure abiotic stress is critical, as it enables successful host infection and the establishment of an intricate regulatory network that governs fungal development, pathogenesis, and abiotic stress response [51,52]. Fungi have developed a sophisticated defense mechanism against oxidative stress, utilizing both enzymatic and non-enzymatic scavengers, growth restriction, DNA restoration, and secondary compounds for protection [53,54]. The present study investigated the cloning and functional characterization of the *AaBemA* gene, which is crucial for ROS accumulation and detoxification in *A. alternata*. Furthermore, the Δ*AaBemA* mutant still retained a substantial capacity for ROS detoxification during host infection, though it caused necrotic lesions on the host plant similar to the wildtype, suggesting that *AaBemA* is necessary for the accumulation of H_2O_2 and oxidative stress response in this fungus, though it does not impact virulence. Previous studies have elucidated the significance of the *Nox* complex, comprising *AaNoxA*, *AaNoxB*, and *AaNoxR*, in cellular hydrogen peroxide accumulation [19]. Mutant strains without *AaNoxA*, *AaNoxB*, or *AaNoxR* were notably more sensitive to various ROS-generating oxidants compared to the wildtype strain in the tangerine pathotype of *A. alternata*. Additionally, the *Nox* mutants displayed reduced sporulation, increased chitin

content, and were incapable of penetrating the citrus host. Therefore, the present study significantly advances our understanding of the role of *AaBemA* in ROS accumulation and tolerance, unraveling its unique contributions within the *A. alternata* fungal system, which contributes to a deeper comprehension of the molecular mechanisms governing oxidative stress response and promotes new avenues for potential interventions targeting ROS management in phytopathogenic fungi. Collectively, all these observations point towards the necessity of *Nox* for the accumulation of hydrogen peroxide and the response to oxidative stress in *A. alternata* as well as the importance of *AaBemA* in this process.

Our previous studies have demonstrated that the thioredoxin (*AaTrr1*, *AaTsa1*) and glutathione (*AaGpx3*, *AaGlr1*) systems, which are adherents of *AaYap1*, distinctly affect fungal development, ROS tolerance, and the virulence of *A. alternata* [23,36]. The study provides compelling evidence that the reduced growth and conidiation observed in the *AaTrr1* or *AaGlr1* deletion mutants can be restored by the addition of glutathione, emphasizing the pivotal role of glutathione in these processes. Moreover, the investigation delves into the susceptibility of deletion mutants to oxidants, showcasing their impaired H_2O_2 detoxification capabilities and resulting in smaller lesions on citrus leaves. This was further supported by the observed upregulation of mutant sulfur metabolism pathway-related genes in the gene targeted deletion mutants, where the glutathione-mediated reduction in thiols and disulfide bonds of proteins is counteracted by glutathione (GRX) and thioredoxin (TRX), respectively [55]. Further investigation of critical genes and pathways related to ROS stress tolerance was conducted through a comparative transcriptome analysis of oxidant-sensitive mutants. The analysis revealed the upregulation of various genes involved in glutathione metabolism, cellular detoxification, abiotic stress response, and osmotic stress response, in both oxidant-sensitive mutants and wildtype under oxidative stress. Such findings indicated that cells have evolved mechanisms to counteract the harmful effects of ROS, including the upregulation of genes related to glutathione metabolism and abiotic stress response [56].

Antioxidant systems play a key role in ROS dynamics of the host–pathogen interactions [52,57,58]. To explore the regulatory mechanism related to ROS tolerance in *A. alternata*, the study compared the transcriptome of antioxidant mutants (Δ*AaBemA*, Δ*AaNoxB*, Δ*AaYap1*, Δ*AaTsa1*, Δ*AaTrr1*, Δ*AaGlr1*), wildtype treated with H_2O_2, wildtype during infection, and wildtype under various stresses. The study employed an in-depth comparative enrichment analysis of GO terms and KEGG pathways based on the transcriptome data of numerous ROS-sensitive mutants, with an aim to more elaborately explore the influence of antioxidant mutants on gene expression. Interestingly, this study found significant influence of key genes involved in glutathione metabolism, attributed to the inactivation of *AaBemA*, *AaNoxB*, *AaTrr1*, *AaGlr1*, *AaYap1*, and *A. alternata* wildtype under ROS stress. Glutathione, an important metabolite in eukaryotes, plays a key role in protecting cells from oxidative damage through direct scavenging of various oxidants [59,60]. We also found that significant impacts of inactivation of *AaBemA*, *AaNoxB*, *AaTrr1*, and *AaGlr1* on the expression of genes enriched in various crucial molecular functions and pathways such as oxidoreductase activity, transmembrane transporter activity, and multiple metabolic pathways related to the regulation of ROS tolerance, providing insights into ROS detoxification and NADPH oxidase-mediated responses.

5. Conclusions

In conclusion, this study explored the regulatory mechanisms of ROS tolerance in *A. alternata* by analyzing transcriptomes of antioxidant mutants (Δ*AaBemA*, Δ*AaNoxB*, Δ*AaTsa1*, Δ*AaTrr1*, Δ*AaGlr1*, Δ*AaYap1*). The results demonstrate a significant impact on the transcription profile of *A. alternata*, especially in the glutathione and thioredoxin systems, offering insights into the mutants' sensitivity to ROS and impaired ability to infect citrus [61]. The findings set the stage for future research, advancing our knowledge of the molecular mechanisms underlying fungal pathogenesis and stress responses, and this holds potential implications for refining agricultural practices and enhancing crop protection.

In the future, additional experiments may be conducted to validate the findings obtained from the transcriptomics analysis. These experiments could include further genetic and biochemical studies aimed at confirming the roles of specific genes or proteins within the antioxidant network. Additionally, more comprehensive functional studies could be undertaken to provide a deeper understanding of the regulatory mechanisms through which the identified genes and proteins govern the response to ROS-induced stress. Moreover, our research group is considering the integration of transcriptomics data with other omics datasets, such as proteomics or metabolomics, to achieve a more holistic comprehension of the regulatory network and the intricate interactions among various components [62].

Supplementary Materials: The following supporting information can be downloaded at: https://www.mdpi.com/article/10.3390/agronomy13112735/s1.

Author Contributions: Conceptualization, X.L. and Y.G.; methodology, X.L., B.Z. and Y.G.; software, Y.G.; validation, X.L., Q.N. and Y.G.; formal analysis, Y.G.; investigation, Y.G.; resources, Y.G.; data curation, X.L., Q.N., J.K. and Y.G.; writing—original draft preparation, X.L., Q.N., J.K., X.Z., B.Z., L.L., C.J. and Y.G.; writing—review and editing, X.L., Q.N., J.K., X.Z., B.Z., L.L., C.J. and Y.G.; visualization, Y.G.; supervision, C.J. and Y.G.; project administration, Y.G.; funding acquisition, Y.G. All authors have read and agreed to the published version of the manuscript.

Funding: This work was supported by grants from the Fundamental Research Funds for the Central Universities (BLX202162) and National Natural Science Foundation of China (32001847).

Institutional Review Board Statement: Not applicable.

Informed Consent Statement: Not applicable.

Data Availability Statement: The biological project login number PRJNA962067 has been assigned to all of the RNA Seq Ilumina data that has been deposited at NCBI. Raw sequence data for transcriptome analysis can be downloaded from the sequence read archive (SRA) of NCBI for the *Alternaria alternata* wildtype (WT) strain Z7: SRR12147525, SRR12147536, SRR12147537; Δ*AaBemA* mutant: SRR24351791, SRR24502884, SRR24502952; Δ*AaNoxB* mutant: SRR24310565, SRR24310856, SRR24313415; Δ*AaTrr1* mutant: SRR24351282, SRR24502494, SRR24502609; Δ*AaTsa1* mutant: SRR24350688, SRR24318093, SRR24350987; Δ*AaGlr1* mutant: SRR24316137, SRR24316136, SRR24316216.

Acknowledgments: We would like to express our gratitude to Hongye Li, Xuepeng Sun, Mingshuang Wang, Haijie Ma, Yanan Chen, and Huilan Fu for their insightful discussions and insightful comments on this work. In addition, we would like to thank the members of the Hongye Li Laboratory at Zhejiang University for their valuable discussion.

Conflicts of Interest: The authors declare no conflict of interest.

Abbreviations

ROS: Reactive Oxygen Species; SODs: Superoxide Dismutases; Nox: NADPH Oxidase; H_2O_2: Hydrogen Peroxide; GFP: Green Fluorescent Protein; NADPH: Nicotinamide adenine dinucleotide phosphate; OMICS: Comprehensive research areas including genomics, proteomics, and metabolomics; Genetic complementation: Restoring a defective gene's function with a functional copy; Transcriptomes: The complete set of RNA transcripts in an organism; Abiotic stimulus: Non-living environmental factors affecting an organism.

References

1. Burdon, J.J.; Thrall, P.H. Coevolution of plants and their pathogens in natural habitats. *Science* **2009**, *324*, 755–756. [CrossRef]
2. Timilsina, S.; Potnis, N.; Newberry, E.A.; Liyanapathiranage, P.; Iruegas-Bocardo, F.; White, F.F.; Goss, E.M.; Jones, J.B. Xanthomonas diversity, virulence and plant–pathogen interactions. *Nat. Rev. Microbiol.* **2020**, *18*, 415–427. [CrossRef]
3. Suzuki, N.; Rivero, R.M.; Shulaev, V.; Blumwald, E.; Mittler, R. Abiotic and biotic stress combinations. *New Phytol.* **2014**, *203*, 32–43. [CrossRef]
4. Czarnockaa, W.; Karpińskia, S. Friend or foe? Reactive oxygen species production, scavenging and signaling in plant response to environmental stresses. *Free Radic. Biol. Med.* **2018**, *122*, 4–20. [CrossRef]

5. Balint-Kurti, P. The plant hypersensitive response: Concepts, control and consequences. *Mol. Plant Pathol.* **2019**, *20*, 1163–1178. [CrossRef]
6. Jeyaraj, A.; Elango, T.; Chen, X.; Zhuang, J.; Wang, Y.; Li, X. Advances in understanding the mechanism of resistance to anthracnose and induced defence response in tea plants. *Mol. Plant Pathol.* **2023**, *24*, 1330–1346. [CrossRef]
7. Wang, W.; Chen, D.; Zhang, X.; Liu, D.; Cheng, Y.; Shen, F. Role of plant respiratory burst oxidase homologs in stress responses. *Free Radic. Res.* **2018**, *52*, 826–839. [CrossRef]
8. Tang, D.; Wang, G.; Zhou, J.-M. Receptor kinases in plant-pathogen interactions: More than pattern recognition. *Plant Cell* **2017**, *29*, 618–637. [CrossRef]
9. Zipfel, C.; Robatzek, S. Pathogen-associated molecular pattern-triggered immunity: Veni, vidi…? *Plant Physiol.* **2010**, *154*, 551–554. [CrossRef]
10. Waszczak, C.; Carmody, M.; Kangasjärvi, J. Reactive oxygen species in plant signaling. *Annu. Rev. Plant Biol.* **2018**, *69*, 209–236. [CrossRef]
11. Vera-Estrella, R.; Barkla, B.J.; Higgins, V.J.; Blumwald, E. Plant defense response to fungal pathogens (activation of host-plasma membrane H+−ATPase by elicitor-induced enzyme dephosphorylation). *Plant Physiol.* **1994**, *104*, 209–215. [CrossRef]
12. Benkő, P.; Gémes, K.; Fehér, A. Polyamine Oxidase-Generated Reactive Oxygen Species in Plant Development and Adaptation: The Polyamine Oxidase—NADPH Oxidase Nexus. *Antioxidants* **2022**, *11*, 2488. [CrossRef]
13. Bleau, J.R.; Spoel, S.H. Selective redox signaling shapes plant–pathogen interactions. *Plant Physiol.* **2021**, *186*, 53–65. [CrossRef]
14. Bhattacharjee, S. Reactive oxygen species and oxidative burst: Roles in stress, senescence and signal transducation in plants. *Curr. Sci.* **2005**, *89*, 1113–1121.
15. Hückelhoven, R. Cell wall–associated mechanisms of disease resistance and susceptibility. *Annu. Rev. Phytopathol.* **2007**, *45*, 101–127. [CrossRef] [PubMed]
16. Kotchoni, S.O.; Gachomo, E.W. The reactive oxygen species network pathways: An essential prerequisite for perception of pathogen attack and the acquired disease resistance in plants. *J. Biosci.* **2006**, *31*, 389–404. [CrossRef]
17. Greenberg, J.T. Programmed cell death: A way of life for plants. *Proc. Natl. Acad. Sci. USA* **1996**, *93*, 12094–12097. [CrossRef] [PubMed]
18. Bettini, P.P.; Cosi, E.; Bindi, D.; Buiatti, M. Reactive oxygen species metabolism in plants: Production, detoxification and signaling in the stress response. *Plant Stress* **2008**, *2*, 28–39.
19. Yang, S.L.; CHUNG, K.R. The NADPH oxidase-mediated production of hydrogen peroxide (H_2O_2) and resistance to oxidative stress in the necrotrophic pathogen Alternaria alternata of citrus. *Mol. Plant Pathol.* **2012**, *13*, 900–914. [CrossRef]
20. Chung, K.-R. Stress response and pathogenicity of the necrotrophic fungal pathogen Alternaria alternata. *Scientifica* **2012**, *2012*, 635431. [CrossRef] [PubMed]
21. Kumari, P.; Gupta, A.; Yadav, S. Thioredoxins as molecular players in plants, pests, and pathogens. In *Plant-Pest Interactions: From Molecular Mechanisms to Chemical Ecology*; Springer: Singapore, 2021; pp. 107–125.
22. Villani, A.; Tommasi, F.; Paciolla, C. The arbuscular mycorrhizal fungus Glomus viscosum improves the tolerance to verticillium wilt in artichoke by modulating the antioxidant defense systems. *Cells* **2021**, *10*, 1944. [CrossRef] [PubMed]
23. Ma, H.; Wang, M.; Gai, Y.; Fu, H.; Zhang, B.; Ruan, R.; Chung, K.-R.; Li, H. Thioredoxin and glutaredoxin systems required for oxidative stress resistance, fungicide sensitivity, and virulence of Alternaria alternata. *Appl. Environ. Microbiol.* **2018**, *84*, e00086-18. [CrossRef] [PubMed]
24. Foyer, C.H.; Noctor, G. Redox homeostasis and antioxidant signaling: A metabolic interface between stress perception and physiological responses. *Plant Cell* **2005**, *17*, 1866–1875. [CrossRef]
25. Gelhaye, E.; Rouhier, N.; Navrot, N.; Jacquot, J.-P. The plant thioredoxin system. *Cell. Mol. Life Sci.* **2005**, *62*, 24–35. [CrossRef]
26. Thon, M.; Al-Abdallah, Q.; Hortschansky, P.; Brakhage, A.A. The thioredoxin system of the filamentous fungus Aspergillus nidulans: Impact on development and oxidative stress response. *J. Biol. Chem.* **2007**, *282*, 27259–27269. [CrossRef] [PubMed]
27. Mukwevho, E.; Ferreira, Z.; Ayeleso, A. Potential role of sulfur-containing antioxidant systems in highly oxidative environments. *Molecules* **2014**, *19*, 19376–19389. [CrossRef]
28. Gellert, M.; Hossain, M.F.; Berens, F.J.F.; Bruhn, L.W.; Urbainsky, C.; Liebscher, V.; Lillig, C.H. Substrate specificity of thioredoxins and glutaredoxins–towards a functional classification. *Heliyon* **2019**, *5*, e02943. [CrossRef]
29. Seco-Cervera, M.; González-Cabo, P.; Pallardó, F.V.; Romá-Mateo, C.; García-Giménez, J.L. Thioredoxin and glutaredoxin systems as potential targets for the development of new treatments in Friedreich's ataxia. *Antioxidants* **2020**, *9*, 1257. [CrossRef]
30. Woudenberg, J.; Groenewald, J.; Binder, M.; Crous, P. Alternaria redefined. *Stud. Mycol.* **2013**, *75*, 171–212. [CrossRef]
31. Meena, M.; Samal, S. Alternaria host-specific (HSTs) toxins: An overview of chemical characterization, target sites, regulation and their toxic effects. *Toxicol. Rep.* **2019**, *6*, 745–758. [CrossRef]
32. Tsuge, T.; Harimoto, Y.; Akimitsu, K.; Ohtani, K.; Kodama, M.; Akagi, Y.; Egusa, M.; Yamamoto, M.; Otani, H. Host-selective toxins produced by the plant pathogenic fungus Alternaria alternata. *FEMS Microbiol. Rev.* **2013**, *37*, 44–66. [CrossRef]
33. Masunaka, A.; Ohtani, K.; Peever, T.; Timmer, L.; Tsuge, T.; Yamamoto, M.; Yamamoto, H.; Akimitsu, K. An isolate of Alternaria alternata that is pathogenic to both tangerines and rough lemon and produces two host-selective toxins, ACT-and ACR-toxins. *Phytopathology* **2005**, *95*, 241–247. [CrossRef]

34. Huang, F.; Fu, Y.; Nie, D.; Stewart, J.E.; Peever, T.L.; Li, H. Identification of a novel phylogenetic lineage of Alternaria alternata causing citrus brown spot in China. *Fungal Biol.* **2015**, *119*, 320–330. [CrossRef] [PubMed]
35. Li, L.; Ma, H.; Zheng, F.; Chen, Y.; Wang, M.; Jiao, C.; Li, H.; Gai, Y. The transcription regulator ACTR controls ACT-toxin biosynthesis and pathogenicity in the tangerine pathotype of Alternaria alternata. *Microbiol. Res.* **2021**, *248*, 126747. [CrossRef]
36. Yang, S.L.; Yu, P.L.; Chung, K.R. The glutathione peroxidase-mediated reactive oxygen species resistance, fungicide sensitivity and cell wall construction in the citrus fungal pathogen A lternaria alternata. *Environ. Microbiol.* **2016**, *18*, 923–935. [CrossRef] [PubMed]
37. de Oya, I.G.; Jiménez-Gutiérrez, E.; Gaillard, H.; Molina, M.; Martín, H.; Wellinger, R.E. Manganese Stress Tolerance Depends on Yap1 and Stress-Activated MAP Kinases. *Int. J. Mol. Sci.* **2022**, *23*, 15706. [CrossRef]
38. Chen, L.-H.; Tsai, H.-C.; Yu, P.-L.; Chung, K.-R. A major facilitator superfamily transporter-mediated resistance to oxidative stress and fungicides requires Yap1, Skn7, and MAP kinases in the citrus fungal pathogen Alternaria alternata. *PLoS ONE* **2017**, *12*, e0169103. [CrossRef]
39. Chen, L.-H.; Yang, S.L.; Chung, K.-R. Resistance to oxidative stress via regulating siderophore-mediated iron acquisition by the citrus fungal pathogen Alternaria alternata. *Microbiology* **2014**, *160*, 970–979. [CrossRef]
40. Wang, M.; Sun, X.; Yu, D.; Xu, J.; Chung, K.; Li, H. Genomic and transcriptomic analyses of the tangerine pathotype of Alternaria alternata in response to oxidative stress. *Sci. Rep.* **2016**, *6*, srep32437. [CrossRef] [PubMed]
41. Bolger, A.M.; Lohse, M.; Usadel, B. Trimmomatic: A flexible trimmer for Illumina sequence data. *Bioinformatics* **2014**, *30*, 2114–2120. [CrossRef]
42. Kim, D.; Langmead, B.; Salzberg, S.L. HISAT: A fast spliced aligner with low memory requirements. *Nat. Methods* **2015**, *12*, 357–360. [PubMed]
43. Anders, S.; Pyl, P.T.; Huber, W. HTSeq—A Python framework to work with high-throughput sequencing data. *Bioinformatics* **2015**, *31*, 166–169. [PubMed]
44. Blin, K.; Shaw, S.; Steinke, K.; Villebro, R.; Ziemert, N.; Lee, S.Y.; Medema, M.H.; Weber, T. antiSMASH 5.0: Updates to the secondary metabolite genome mining pipeline. *Nucleic Acids Res.* **2019**, *47*, W81–W87. [PubMed]
45. Krzywinski, M.; Schein, J.; Birol, I.; Connors, J.; Gascoyne, R.; Horsman, D.; Jones, S.J.; Marra, M.A. Circos: An information aesthetic for comparative genomics. *Genome Res.* **2009**, *19*, 1639–1645.
46. Gu, Z.; Eils, R.; Schlesner, M. Complex heatmaps reveal patterns and correlations in multidimensional genomic data. *Bioinformatics* **2016**, *32*, 2847–2849. [PubMed]
47. Guy, L.; Roat Kultima, J.; Andersson, S.G. genoPlotR: Comparative gene and genome visualization in R. *Bioinformatics* **2010**, *26*, 2334–2335.
48. Langfelder, P.; Horvath, S. WGCNA: An R package for weighted correlation network analysis. *BMC Bioinform.* **2008**, *9*, 1–13.
49. Fu, H.; Chung, K.-R.; Liu, X.; Li, H. Aaprb1, a subtilsin-like protease, required for autophagy and virulence of the tangerine pathotype of Alternaria alternata. *Microbiol. Res.* **2020**, *240*, 126537.
50. Sun, X.; Wang, J.; Feng, D.; Ma, Z.; Li, H. PdCYP51B, a new putative sterol 14α-demethylase gene of Penicillium digitatum involved in resistance to imazalil and other fungicides inhibiting ergosterol synthesis. *Appl. Microbiol. Biotechnol.* **2011**, *91*, 1107–1119.
51. Mehta, A.; Brasileiro, A.C.; Souza, D.S.; Romano, E.; Campos, M.A.; Grossi-de-Sá, M.F.; Silva, M.S.; Franco, O.L.; Fragoso, R.R.; Bevitori, R. Plant–pathogen interactions: What is proteomics telling us? *FEBS J.* **2008**, *275*, 3731–3746.
52. Deboever, E.; Deleu, M.; Mongrand, S.; Lins, L.; Fauconnier, M.-L. Plant–pathogen interactions: Underestimated roles of phyto-oxylipins. *Trends Plant Sci.* **2020**, *25*, 22–34. [PubMed]
53. Lushchak, V.I. Adaptive response to oxidative stress: Bacteria, fungi, plants and animals. *Comp. Biochem. Physiol. Part C Toxicol. Pharmacol.* **2011**, *153*, 175–190.
54. Zadrąg-Tęcza, R.; Maślanka, R.; Bednarska, S.; Kwolek-Mirek, M. Response mechanisms to oxidative stress in yeast and filamentous fungi. In *Stress Response Mechanisms in Fungi*; Springer: Cham, Switzerland, 2018; pp. 1–34.
55. Perween, N.; Pekhale, K.; Haval, G.; Mittal, S.; Ghaskadbi, S.; Ghaskadbi, S.S. A novel thioredoxin glutathione reductase from evolutionary ancient metazoan Hydra. *Biochem. Biophys. Res. Commun.* **2022**, *637*, 23–31.
56. Pandey, A.K.; Gautam, A. Stress responsive gene regulation in relation to hydrogen sulfide in plants under abiotic stress. *Physiol. Plant.* **2020**, *168*, 511–525.
57. Mandal, S.; Acharya, P.; Kar, I. Reactive oxygen species signaling in eggplant in response to Ralstonia solanacearum infection. *J. Plant Pathol.* **2014**, *96*, 525–534.
58. Zhang, W.; Wang, Z.; Dan, Z.; Zhang, L.; Xu, M.; Yang, G.; Chai, M.; Li, Z.; Xie, H.; Cong, L. Transcriptome Analysis of Fusarium Root-Rot-Resistant and-Susceptible Alfalfa (*Medicago sativa* L.) Plants during Plant–Pathogen Interactions. *Genes* **2022**, *13*, 788. [PubMed]
59. Chai, Y.-C.; Mieyal, J.J. Glutathione and Glutaredoxin—Key Players in Cellular Redox Homeostasis and Signaling. *Antioxidants* **2023**, *12*, 1553.
60. Ali, S.S.; Ahsan, H.; Zia, M.K.; Siddiqui, T.; Khan, F.H. Understanding oxidants and antioxidants: Classical team with new players. *J. Food Biochem.* **2020**, *44*, e13145. [CrossRef]

61. Hajam, Y.A.; Rani, R.; Ganie, S.Y.; Sheikh, T.A.; Javaid, D.; Qadri, S.S.; Pramodh, S.; Alsulimani, A.; Alkhanani, M.F.; Harakeh, S. Oxidative stress in human pathology and aging: Molecular mechanisms and perspectives. *Cells* **2022**, *11*, 552.
62. O'Connor, L.M.; O'Connor, B.A.; Lim, S.B.; Zeng, J.; Lo, C.H. Integrative multi-omics and systems bioinformatics in translational neuroscience: A data mining perspective. *J. Pharm. Anal.* **2023**, *13*, 836–850.

Disclaimer/Publisher's Note: The statements, opinions and data contained in all publications are solely those of the individual author(s) and contributor(s) and not of MDPI and/or the editor(s). MDPI and/or the editor(s) disclaim responsibility for any injury to people or property resulting from any ideas, methods, instructions or products referred to in the content.